CHROMENE BASED COMPOUNDS TO TREAT MULTIDRUG RESISTANT CANCER

A THESIS SUBMITTLED
TO THE FACULTY OF
UNIVERSITY OF MINNESOTA
BY

DENISE NICOLE CASEMORE

IN PARTIAL FULFILLMENT OF THE REQUIREMENTS
FOR THE DEGREE OF
MASTER OF SCIENCE

Dr. CHENGGUO XING, ADVISOR

APRIL 2016

Acknowledgements

"Our greatest weakness lies in giving up. The most certain way to succeed is always to try just one more time." – Thomas A. Edison

The most difficult thing for me is to ask for help, so I am very grateful for all the help I have received in these past three years. First and foremost I have to thank my advisor and mentor Dr. Chengguo Xing, who has consistently been supportive and insightful in my research. Dr. Xing has taught me how to ask questions and intelligently design experiments to answer them. He has taught me how to question results and has impressed upon me the importance of experimental reproducibility. Secondly I greatly appreciate the guidance, feedback and encouragement I have received from my fellow medicinal chemistry classmates. I would also like to thank the former and current Xing lab members for their advice and experimental insight, especially Dr. Bo Zhou, Dr. Sreekanth Narayanapillai, Nick Bleeker, Dr. Manohar Puppala, Dr. Yuesheng Dong, and Tengfei Bian. I would like to acknowledge the staff of the medicinal chemistry department, who has provided me with the necessary facilities, materials, and documentation to complete this program. Lastly and most importantly I must acknowledge the support and love I have received from my family throughout this tumultuous journey. I cannot thank my mom enough for never doubting my abilities or intelligence.

Abstract

The Xing lab has explored CXL compounds as cytotoxic anticancer agents in multi-drug resistant leukemic cell lines. CXL compounds have exhibited an increased potency in drug resistant cell lines compared to their parental cell lines. CXL compounds act through the inhibition of the sarco-endoplasmic reticulum calcium ATPase (SERCA). SERCA inhibition causes cell death through an increase in cytosolic calcium levels, ER stress, and triggering the unfolded protein response. The binding site of CXL compounds on SERCA and the identity of other cellular targets have been investigated through photoaffinity labeling with probes CXL039 and CXL037 respectively. Alterations in the synthesis of CXL compounds were also examined to improve the overall yield. Compounds that exhibit the same cytotoxicity profile as CXL compounds were explored through a cell based screen of natural products in HL60 and HL60 doxorubicin resistant cells.

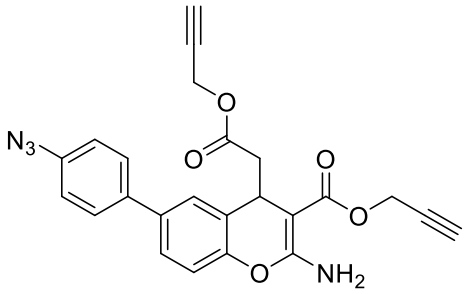

CXL039

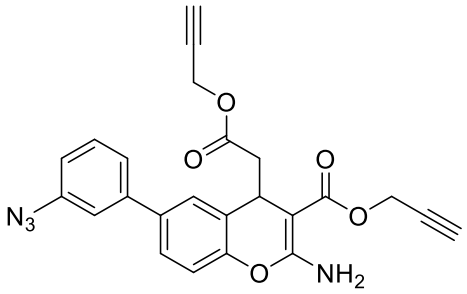

CXL037

Table of contents

List of figures

List of schemes

List of equations

List of abbreviations

ADR	Adriamycin
AMPK	AMP-activated kinase
ATP	Adenosine triphosphate
BCA	Bicinchoninic acid
Bcl-2	B-cell lymphoma-2
BHQ	2,5-di-*tert*-butylhydroquinone
BSA	Bovine serum albumin
C2	Camptothecin
CaMKKβ	Calcium/calmodulin-dependent kinase kinase-β
CPA	Cyclopiazonic acid
DMSO	Dimethylsulfoxide
DNR	Daunorubicin
DOX	Doxorubicin
ER	Endoplasmic reticulum
ERS	Endoplasmic reticulum stress
FBS	Fetal bovine serum
HRP	Horse radish peroxidase
IP_3R	Inositol triphosphate receptor
MDR	Multidrug resistance
MEFs	Murine embryonic fibroblasts
MOMP	Mitochondrial outer membrane permeablization
MOPS	3-morpholinopropane-1-sulfonic acid
MX	Mitoxantrone

PBST	Phosphate buffered saline TWEEN-20
PEG	Polyethylene glycol
P-gp	P-glycoprotein
PMCA1	Plasma membrane calcium transporting ATPase 1
PSA	Prostate surface antigen
PVDF	Polyvinylidene difluoride
RyR	Ryanodine receptor
SDS-PAGE	Sodium dodecyl sulfate polyacrylamide gel electrophoresis
SERCA	Sarco/endoplasmic reticulum calcium ATPase
TBTA	Tris-(benzyltriazolylmethyl)amine
TCEP	Tris-(2-carboxyethyl)phosphine
TG	Thapsigargin
UPR	Unfolded protein response
VLB	Vinblastine

Chapter 1: SERCA as a target to treat multi-drug resistant cancer

1.1 Introduction

Tumors consist of heterogeneous cell populations. These populations contain cells that are drug sensitive or resistant to anticancer therapies. Exposure to first line chemotherapeutics can effectively eliminate drug sensitive cells, while not, or less effectively, harming the drug resistant cells. Drug resistant tumors are then the result of these resistant cells. When these tumors are resistant to multiple structurally and functionally dissimilar chemotherapeutics, they are considered multidrug resistant.[1] Multidrug resistance (MDR) can arise from a cancer cell's inherent genetic or epigenetic resistance to anticancer drugs.[2] MDR also results from mutations or activation of adaptive response mechanisms upon exposure to chemotherapy. These adaptive response mechanisms include an increase in the chemotherapeutic target or activation of complementary signaling pathways.[3] Other mechanisms of drug resistance include an over expression of antiapoptotic factors, such as the Bcl-2 family members, or an increased expression in drug efflux pumps, such as the ATP-binding cassette transporter proteins. An increase in cellular repair mechanisms and alterations in drug metabolism can also contribute to drug resistance.[3] A strategy to combat these resistances is to discover new cellular targets. One relatively new target for treating cancer, particularly drug resistant cancer, is the sarco-endoplasmic reticulum calcium ATPase (SERCA).

1.2 SERCA as a target for cancer therapy

SERCA is a p-type ATPase located in the sarco-endoplasmic reticulum of all cells. SERCA uses the energy from the hydrolysis of ATP to pump calcium ions from the

cytosol against the concentration gradient into endoplasmic reticulum (ER). The ER is the central intracellular calcium storage organelle, and SERCA is the integral protein that transports calcium ions into the ER. SERCA, along with other calcium channels/pumps are critical in the regulation of cellular calcium homeostasis. The concentration of cytosolic calcium controls cell proliferation, gene transcription, cell death, and many other cellular processes. In normal cells, resting cytosolic calcium levels are at nanomolar concentrations, whereas concentrations in the ER lumen are in the micromolar range, and extracellular calcium concentrations are in the millimolar range. Alterations in these resting calcium concentrations can represent a disease state due to chemical or signal transduction changes in regulation.[4]

SERCA is encoded in several isoforms, *ATP2A1, 2A2, 2A3*. Alternative splicing of SERCA these genes yields even more isoforms of SERCA proteins.[5] Typically SERCA isoforms share ~75% sequence homology.[6] Expression of SERCA isoforms is cell type dependent. SERCA1a and 1b are found primarily in skeletal muscle. SERCA2a is mostly found in cardiomyocytes. SERCA2b is found in all cell types. SERCA2c is found in non-muscle cells. SERCA3 has six known splice isoforms and is co-expressed with SERCA2b in many tissues. SERCA3 expression is also cell type dependent with a higher expression in cells of hematopoietic origin.[5] SERCA2b is the most common SERCA isoform and it has the highest calcium affinity, whereas SERCA3 has the lowest calcium affinity.[5, 7]

SERCA inhibition can increase cytosolic calcium levels resulting in cellular death through apoptosis, necrosis, and autophagy. Calcium is released from the ER by inositol-1,4,5-phosphat-receptor (IP_3R) and ryanodine receptor (RyR) or by calcium leakage, via SERCA inhibition. Calcium leakage from the ER can lead to calcium uptake by the mitochondria.[8] An increase in mitochondrial calcium levels can lead to permeablization of the mitochondrial outer membrane (MOMP) by pro-apoptotic Bax and Bak, followed by release of cytochrome C, which activates caspase 9 resulting in apoptosis.[8] An increase in cytosolic calcium concentration can also activate calcineurin, which then dephosphorylates Bad. Dephosphorylated Bad inhibits anti-apoptotic Bcl-2 leading to similar MOMP followed by apoptosis.[9] An increase in cytosolic calcium concentration also triggers other forms of cell death, including necrosis, necrotic-like-apoptosis, and autophagy. Necrotic hallmarks, such as mitochondrial swelling, cell volume increase, and rupture of the plasma membrane, were observed when murine embryonic fibroblasts (MEFs), deficient in proapoptotic Bak and Bax, were treated with thapsigargin (TG), a potent and non-selective SERCA inhibitor.[10] An overload in the mitochondrial transmembrane potential, due to calcium uptake from ER release, causes an opening of the mitochondrial permeability transition pore, which induces mitochondrial swelling as seen in necrosis.[11] Mitochondrial swelling can also cause MOMP, releasing cytochrome C and subsequently activate the apoptotic pathway independently of Bak and Bax, creating a hybrid of necrosis and apoptosis induced cell death.[10, 12] An increase in the cytosolic calcium concentration also stimulates calcium/calmodulin-dependent kinase kinase-β (CaMKKβ), which activates AMP-activated kinase (AMPK) that in turn inhibits

mTORC1 inducing autophagy and cell death.[13] TG inhibition of SERCA induced CaMKKβ/AMPK autophagy in HeLa and MCF-7 cells.[14]

In addition to an increase in cytosolic calcium concentration, depletion of calcium in the ER can also serve as a direct trigger to programmed cell death. Specifically, a decrease of calcium concentration in the ER will lead to ER stress response (ERS) and unfolded protein response (UPR). As observed in HeLa cells ER stress can lead to cleavage of pro-caspase 12 by m-calpain, which then activates subsequent caspases resulting in apoptotic cell death.[11, 15] ER calcium levels are needed for the function of calreticulin and calnexin, which are involved in protein folding. Depletion of ER calcium stores lead to an increase of misfolded proteins, resulting in ER stress response or UPR.[16] UPR activates pathways that decrease protein synthesis, activate autophagy, and increase protein degradation and folding.[17] Prolonged activation of these responses leads to apoptosis.[18]

In addition to the direct initiation of programmed cell death via SERCA inhibition, a cellular gene expression and function based high throughput screen identified SERCA as a key regulatory protein of Notch1 signaling. SERCA inhibitors, such as, TG, were identified to preferentially target Notch1 driven malignancies. SERCA's pivotal role in cellular calcium regulation, and interaction with Notch1, makes it a potential target in development of selective inhibitors for cancer therapies.

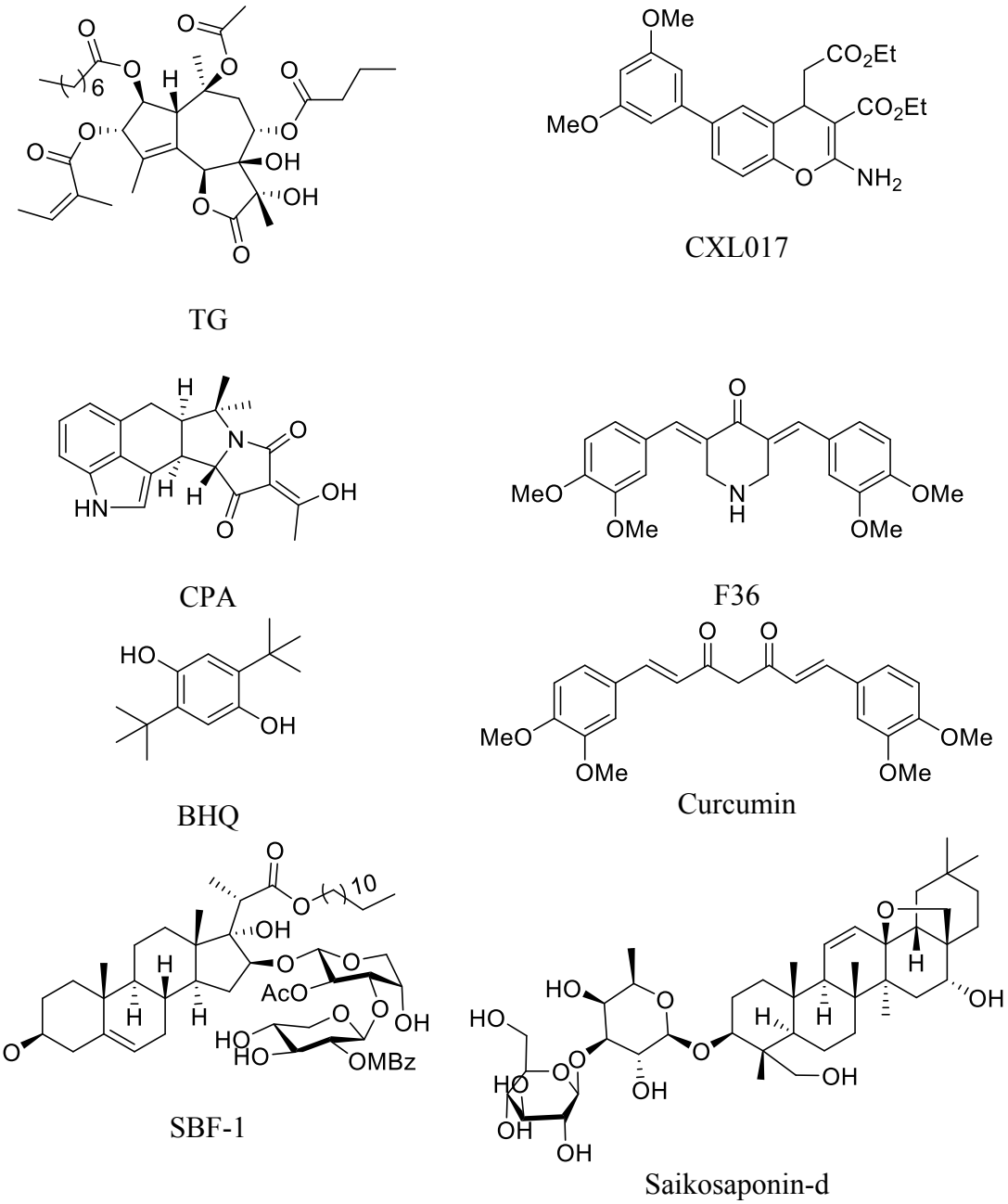

Figure 1.1 Structure of SERCA inhibitors

1.3 Known SERCA inhibitors

A number of SERCA inhibitors have been identified with different potency, selectivity and preferred binding states. The most potent inhibitor of SERCA known to

date is TG. TG is a sesquiterpene lactone isolated from the plant *Thapsia garganica*. TG treatment increases the cytosolic calcium concentration, while it depletes ER calcium stores via SERCA inhibition. TG also inhibits SERCA in stoichiometric quantities affecting the calcium transport and ATPase activity of SERCA.[19] TG inhibits the calcium free state of SERCA in low nanomolar concentrations forming a dead end complex.[20] At low nanomolar concentrations, TG selectively inhibits SERCA over other calcium transport pumps. TG binds SERCA in the transmembrane helices M3, M5, and M7 by forming hydrogen bonds and hydrophobic interactions. Even though SERCA isoforms have a high percentage of sequence and presumably structure homology, they have different sensitivities for TG inhibition. TG potently inhibits SERCA1b with a K_i of 0.21 ± 0.05nM, SERCA2b 1.3 ± 0.05nM while its K_i for SERCA3a is only 12 ± 6nM. All analogs of TG have proved to be less potent than the parent compound.[19] Cellular treatment with TG at different concentrations leads to both a short term (15min) large cytosolic increase in calcium concentration, resulting in apoptosis, and a long term (48h) minor cytosolic increase in calcium leading to proliferation.[8]

Other selective but less potent inhibitors of SERCA include cyclopiazonic acid (CPA) and 2,5,-di(t-butyl) hydroquinone (BHQ). CPA and BHQ have different inhibitory potency against SERCA isoforms 1b, 2b and 3a. The K_i of CPA inhibition is 90 ± 30nM for SERCA1b, 2.5 ± 0.05μM for SERCA2b and 600± 200nM for SERCA3a. The K_i of BHQ inhibition of SERCA1b is 7 ± 4μM, 2.6 ± 1.3μM for SERCA2b and 1.7± 1μM for SERCA3a.[6] Site-directed mutagenisis demonstrated that CPA and BHQ bind to different sites relative to TG on SERCA. The mutation F256V in SERCA reduced the potency of

TG inhibition 200 fold for SERCA1b, 5 fold for SERCA2b, and 100 fold for SERCA3a. Other inhibitors, CPA and BHQ exhibited little difference in K_i values between the wild type and mutant isoforms.[6] These small molecules bind SERCA in a transmembrane site that differs from TG, but all stabilize SERCA in the low calcium affinity state.[19]

Another SERCA inhibitor, curcumin, a natural product from turmeric, has been investigated in clinical trials for anti-cancer activity towards colorectal cancer.[21] Curcumin inhibits SERCA by stabilizing the E1 conformation with a K_i of 15μM. It binds competitively with ATP and non-competitively with calcium.[19] Curcumin has some selectivity among SERCA isoforms. It inhibits SERCA1b (5.8 ± 1.6μM) and 3a (8.6 ± 2.5μM) with similar K_i values but inhibits SERCA 2b with a significantly decreased potency (53 ± 6μM).[6] F36 is a more active piperdone analog of curcumin and is more effective at inhibiting the proliferation of colorectal cancer cell lines mainly by targeting SERCA2 expression.[22]

Saikosaponin-d (Ssd), a natural triterpenoid saponins isolated from *Bupleurum falcatum L.,* induces autophagy by inhibition of SERCA. SERCA inhibition results in an increase of cytosolic calcium levels leading to ER stress and UPR. Interestingly, Ssd exhibited similar micromolar cytotoxicity in cells deficient in caspase-3/-7/-8 or Bax-Bak, which are typically apoptosis deficient. These findings indicate that the cytotoxicity due to Ssd can circumvent the defect in the apoptotic pathway and could be used in cancers resistant to drugs that target the apoptotic pathway.[23]

Through SERCA inhibition SBF-1, a steroidal glycoside, was found to cause ER stress and UPR in cervical cancer HeLa cells. SBF-1 was found to bind and inhibit the activity of SERCA2 at nanomolar levels, which is elevated in cervical cancers. However, SBF-1 also binds to plasma membrane calcium transporting ATPase 1, PMCA1, which may account for its anticancer potential.[24]

1.4 CXL series as anticancer agents

The Xing's lab has identified a stable derivative of HA 14-1 (sHA 14-1) as a dual inhibitor of both Bcl-2 and SERCA. sHA 14-1 induces cell death through ER stress and calcium release.[25] Exploration of the structure activity relationship of sHA 14-1, led to the discovery of ethyl 2-amino-6-(3,5-dimethoxyphenyl)-4-(2-ethoxy-2-oxoethyl)-4H-chromene-3-carboxylate (CXL017) and subsequent analogues. CXL017 was comparable in cytotoxicity to ABT-737, a Bcl-2 inhibitor, in 11 cancer cell lines. CXL017 revealed a dose dependent increase in PARP cleavage and caspase-3/7 activation in NALM-6 cells.[26] Most interestingly, CXL017 exhibited preferentially cytotoxicity in multi-drug resistant HL60/MX2 and CCRF-CEM/CT cancer cell lines. CXL017 also revealed synergy when combined with standard chemotherapeutics, vincristine, paclitaxel, and mitoxantrone in treating MDR cells.[27] This suggests CXL017 can be combined with these drugs to treat MDR cancer cells. An NCI-60 screen of CXL017 revealed a mean GI_{50} of 1.04μM. It also revealed that CXL017 was more effective in leukemia, colon cancer, melanoma, and breast cancer cells than in renal, ovarian, and non-small-cell lung cancer cells. COMPARE analysis of the screen revealed that CXL017 has a unique mechanism of action, possibly explaining the selectivity for MDR cells.[27]

Interestingly, CXL017 exhibited synergy with the general SERCA inhibitors TG, BHQ, and CPA in inhibition of SERCA activity and in inducing cellular cytotoxicity.[28] In 9 resistant leukemic cell lines CXL compounds remained cytotoxic, but TG lost its cytotoxicity in 5 of the cell lines, 4 of which have an increased expression levels of P-gp, suggesting TG might be a substrate for the efflux pump.[29] CXL compounds along with TG, BHQ, CPA exhibited selective cytotoxicity in HL60/MX2 cells compared to parental HL60, proving SERCA as a target to overcome the drug resistance in these cells.[28] However, the exact binding site/state of SERCA by CXL017 remains to be determined, which may help rationalize the unique activity profile and guide future optimization.

1.5 SERCA expression and intracellular calcium level in cancer cells

Like many proteins, SERCA expression levels are altered in cancers. SERCA3 expression is induced during cell differentiation, but decreased in the tumorigenesis of cancers, such as colon and breast.[30] Expression of SERCA3 and 2b isoforms have been found to differ in normal verses cancer cells in myeloid leukemia, colon carcinoma, breast cancer.[30] Expression of SERCA2 was decreased in squamous cell carcinoma, in addition to colon, lung, colorectal, and thyroid cancers.[31, 32] Expression of SERCA3 is increased in APL cells, but decreased in colorectal carcinoma, gastric carcinoma, and breast cancer.[5, 16, 33] This decrease has been suggested to possibly contribute to the induction of malignancy, and provides evidence that calcium regulation is modified in cancer cells to prevent apoptosis.[16, 34] Alterations in calcium regulation in mice, heterozygous for SERCA2, revealed a significant increased sensitivity toward the development of squamous-cell carcinomas, indicating that alterations in intracellular

calcium regulation can lead to cancer development.[35, 31] SERCA 2b and 3 are often co-expressed in cells and decrease in the expression of one isoform, however, does not necessarily indicate a decrease in both. SERCA 2b and 3 have different turnover rates and calcium affinities making them active at different levels of cytosolic calcium.[30] The remodeling of calcium regulation in cancer cells is still not well understood, but there has to be enough SERCA to maintain ER calcium levels to sustain protein synthesis. Lastly SERCA inhibitors such as TG have caused cytotoxicity in cancer cells with reduced SERCA expression.

Cytosolic calcium levels change in cancer cells due to changes in expression of endoplasmic reticulum membrane proteins, such as SERCA, IP_3R, and Bcl-2 family proteins.[36] IP_3R and SERCA are regulated by anti-apoptotic Bcl-2, which is highly expressed in many cancers. Bcl-2 regulates the release of calcium from the ER via IP_3R to prevent large releases of calcium that can trigger apoptosis to allow small releases that promote proliferation.[36] Bcl-2 modulation of IP_3R has also inhibits autophagy induced by an increase in cytosolic calcium levels.[14] Overexpression of Bcl-2 is observed in MCF-7 breast cancer cells, and has been shown to modulate IP_3R, and decrease calcium in the ER.[31] Additionally Bcl-2 has been implicated in the regulation of SERCA, decreasing the amount of calcium pumped into the ER to prevent releases of calcium sufficient to trigger apoptosis.[8]

1.6 Cell targeting

Targeting SERCA inhibition as a treatment for cancer does not come without

risks. Decrease in ER calcium levels may lead to heart failure if the incubation is not selective.[37] In addition, since different cell types and cancers have different expression levels of SERCA isoforms, isoform-specific inhibitors may be necessary to achieve tissue-targeted therapies.

One alternative strategy explored to target cancer cells is bioconjugation. TG has been coupled with a peptide that can be cleaved by PSA, prostate surface antigen, forming TG prodrugs for prostate cancer. The prodrug should increase the selectivity and decrease the toxicity of TG alone. PSA is a serine protease that has an increased expression in prostate cancer cells and is only active near the prostate at the site of its secretion allowing TG to selectively target prostate cells.[38] The TG prodrug is impenetrable to cell membranes, but once cleaved by PSA, the12-aminododecanoyl linker allows for rapid cellular uptake. The resulting TG analogs are slightly less potent then the parent TG. Currently these prodrugs are in clinical trials for the treatment of prostate cancer.[38, 39]

1.7 Conclusion

SERCA is a new target for chemotherapy, due to its important role in cellular calcium regulation. SERCA inhibition causes an increase in cytosolic calcium concentration that can trigger ERS, UPR, and other pathways, resulting in programmed cell deaths that may differ from the standard cancer therapies. The development of selective and potent SERCA inhibitors have proven to be effective in causing the cytotoxicity of sensitive and resistant cancer cells in vitro, but tissue selectivity and

cardiovascular risk still needs to be assessed in vivo and clinically.

Chapter 2: Improve the synthesis of CXL compounds

2.1 Introduction

Previous investigations by the Xing lab into 4-H-chromene based anticancer candidates (CXL) identified CXL017 as a novel SERCA inhibitor.[25, 28] Further explorations by the Xing lab into the structure activity relationship (SAR) of CXL compounds revealed that their cellular cytotoxicity is sensitive to changes in functional groups at the 3 and 4 positions preferring esters with small, rigid, and lipophilic alkoxy groups (Figure 2.1).[26, 27, 29] These studies also revealed a preference for small and hydrophilic substitutions at the meta- and para- positions on the aryl ring at the 6-position of the CXL scaffold.[40] The lead compound that resulted from these investigations was CXL070. It has propargyl esters at the 3 and 4 positions, and an amino group in the 4′ position on the aryl ring at the 6 position (Figure 2.1).

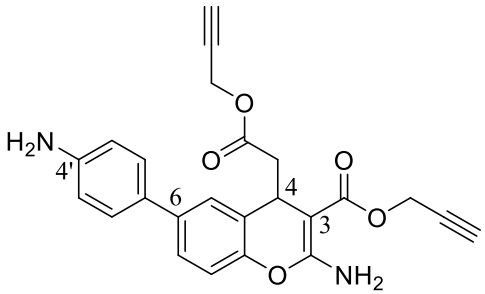

Figure 2.1 Structure of CXL070

CXL070 is cytotoxic across several multidrug resistant (MDR) cancer cell lines including HL60/MX2, HL60/ADR, HL60/DNR, HL60/DOX, K562/DOX, K562/HHT300, CCRF-CEM/C2, CCRF-CEM/VM-1-5, CCRF-CEM/VLB100, with low to submicromolar IC_{50} values.[29] Although these cancer cell lines have different

mechanisms of MDR, down regulation of topoisomerase IIβ (HL60/MX2), target mutation (CCRF-CEM/C2, CCRF-CEM/VM-1-5), an increase in anti-apoptotic Bcl-2 proteins (CCRF-CEM/C2, HL60/MX2), an up-regulation of c-inhibitor of apoptosis (HL60/DOX), or an overexpression of P-gp (HL60/ADR, HL60/DNR, K562/DOX, K562/HHT300, CCRF-CEM/VLB100), CXL070 remains potent across all of them. This suggests that CXL070 targets several key MDR mechanisms and cancer cells are unlikely to become resistant to it, making it a good candidate to treat MDR. The overall yield for the synthesis of CXL070 however is only 25% over 4 steps. In order to improve the yield to make enough of CXL070 for larger scale studies, alterations to the synthetic route were investigated.

2.2 Results and discussion

2.2.1 Revision of the synthetic route of CXL070

The synthesis of CXL070 has previously been reported (Scheme 2.1).[29] The first step in the synthesis of CXL070 is the formation of 6-bromo-2H-chromen-2-one from 2-(dimethylamino)-2-oxoethan-1-ylium and 5-bromo-2-hydroxybenzaldehyde, with an 88% yield. The second step in the synthesis used a Suzuki reaction to cross couple 6-bromo-2H-chromen-2-one and 4-nitro-aryl boronic acid to form 6-(4-nitrophenyl)-2*H*-chromen-2-one. The Suzuki reaction has the lowest yield in the scheme, 58%. The formation of 6-(4-nitrophenyl)-2*H*-chromen-2-one was followed by a reduction to give 6-(4-aminophenyl)-2*H*-chromen-2-one, with a 72% yield. Finally ethyl 2-cyanoacetate was added to 6-(4-aminophenyl)-2*H*-chromen-2-one in the presence propargyl alcohol to

form the final product prop-2-yn-1-yl 2-amino-6-(4-aminophenyl)-4-(2-oxo-2-(prop-2-yn-1-yloxy)ethyl)-4*H*-chromene-3-carboxylate (CXL070), with a 67% yield.

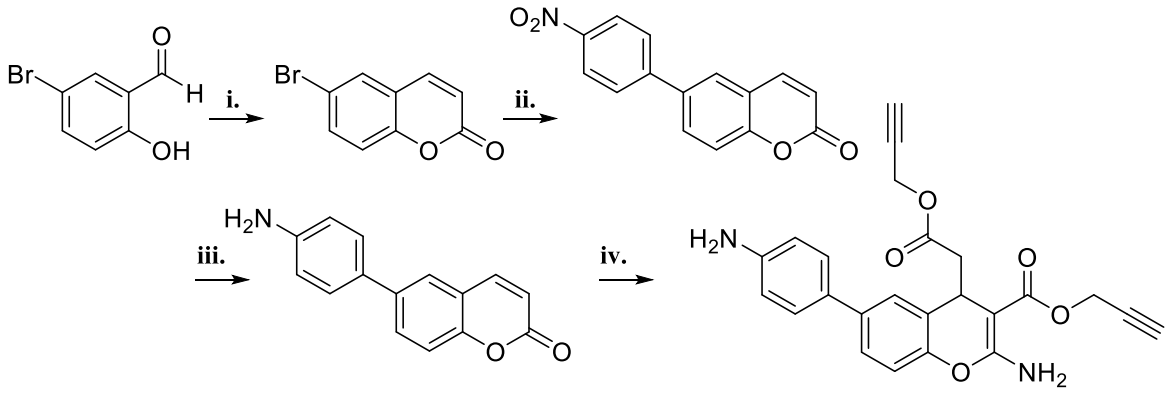

Scheme 2.1 Original synthetic route of CXL070 Reagents and conditions: (i) DMA, $POCl_3$, DCM, 0 °C to 80 °C, 4 h, $NaHCO_3$, 60 °C, 1 h; (ii) 4-nitrophenylboronic acid, $Pd(PPh_3)_4$, K_2CO_3, Toluene:H_2O, 80 °C, 16 h; (iii), Pd/C (10%), NH_4CO_2, MeOH, 6 h, rt (iv) Ethyl cyanoacetate, Na, C_3H_3OH, rt, 24h.

To improve the overall yield of 25%, my focus was placed on optimizing the reaction with the lowest yield, the Suzuki coupling. In the previous synthesis the Suzuki reaction was never optimized for these substrates. The mechanism of a Suzuki cross coupling is illustrated in Figure 2.2. The biaryl cross coupling reaction starts with the oxidative addition of an aryl halide to Pd(0). Transmetalation with an aryl boronic acid species, followed by reductive elimination produces the biaryl product and regenerates Pd(0).[41] Some well demonstrated factors that affect a Suzuki reaction include temperature, time, concentration, bases, solvent, metal catalyst and ligand.[42] Since 1997 two step one pot Suzuki coupling reactions have been reported that generate the aryl boronic acid in situ before cross coupling with an aryl halide or aryl triflate.[43] These

reactions have shown promise in decreasing the need for excess reactants, decreasing reaction temperature, and good yields.

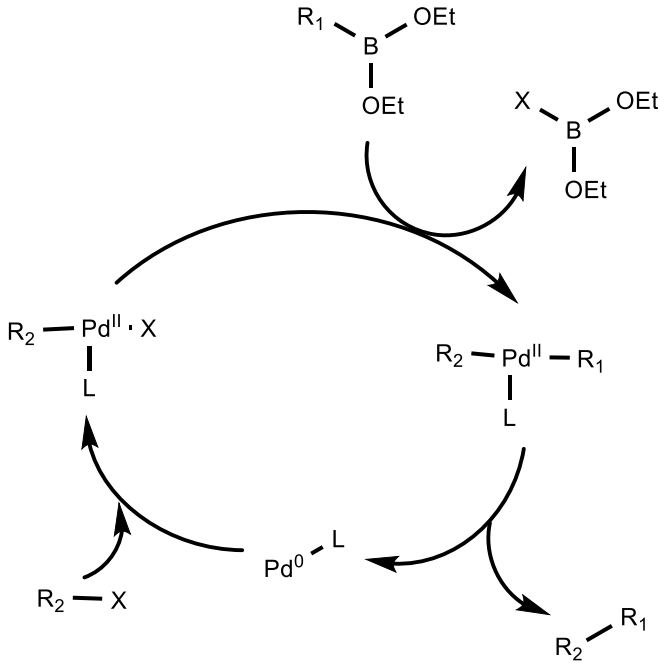

Figure 2.2 Suzuki mechanism X=Br, Cl L=ligand

A one-pot reaction that forms the reactive boronic acid in situ followed by aryl cross coupling was investigated as a replacement for the traditional Suzuki reaction in the synthesis of CXL070.[44] The one-pot reaction conditions used were developed by Molander et al. and use tetrahydroxydiboron, potassium acetate, XPhos, and XPhos-Pd-G2, an X-Phos second generation Buchwald aminobiphenyl palladium chloride precatalyst, to do an in situ Miyaura borylation of a chloro or bromo substituted aromatic compound before the addition of a stronger second base, potassium carbonate, and the second coupling reagent.[44] Catalysts containing biarylphosphine ligands like XPhos have revealed to be more active and have improved efficiency in borylation and cross coupling reactions than previous explored systems.[41] This one-pot reaction eliminated the need of

expensive and degrading bornic species, used small amounts of catalyst and ligand, and eliminated the use of excess starting material.[44]

Scheme 2.2 Two-step one pot cross coupling reaction

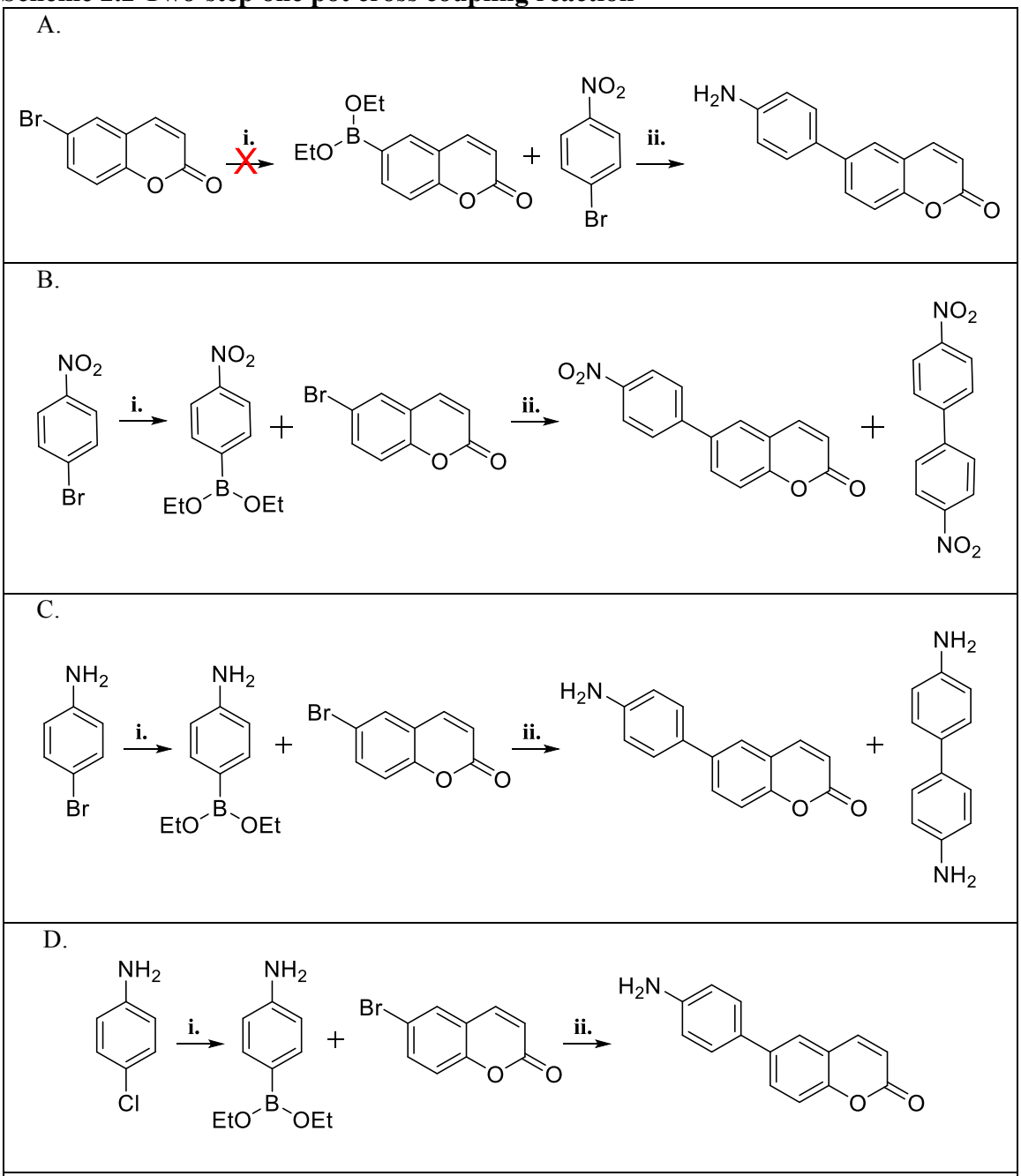

Reagents and conditions: (i) XPhos Pd G2, XPhos, KOAc, $B_2(OH)_4$, EtOH, 80°C, 2h; (ii) K_2CO_3, 80°C, 18h.

Initially 6-bromo-2H-chromen-2-one was investigated as the reagent to undergo the in situ borylation, followed by coupling with 4-bromo-nitrobenzene (Scheme 2.2 A). Efficient cross coupling was previously observed in two step one pot reactions when aryl compounds, with electron rich substituents, formed the boronate intermediate.[45] Unfortunately, the reaction did not occur and the majority of the starting material was recovered. Recovery of the starting material indicated that the first step did not occur, possibly due to slow formation of the boronate intermediate, which can lead to low yields overall.[45] It has been observed that electron withdrawing groups, like nitro groups, on an aryl ring can speed up the initial hydroboration reaction.[46]

In order to facilitate the initial step 4-bromo-nitrobenzene was used to form the in situ borylated product. This led to the formation of the desired coupled product in 48% yield, but a significant amount of self coupling of 4-bromo-nitrobenzene was also observed (Scheme 2.2 B). Self coupling of aryl groups of the aryl boronic acids can occur when the cross coupling reaction occurs slowly.[47] Self coupling can occur more readily when aryl reactants contain electron withdrawing substituents.[47] To reduce the amount of self coupled product 4-bromo-nitrobenzene was replaced with 4-bromo-aniline. Replacing the electron withdrawing nitro group with an electron donating amino group should decrease the amount of self coupling. Using the aniline would also eliminate the need for nitro group reduction in the synthetic route of CXL070.

Replacing 4-bromo-nitrobenzene with 4-bromo-aniline yielded 84%, but again the self coupled product was observed (Scheme 2.2 C). The persistence of self coupling

might be due in part to reactivity of bromobenzne derivatives. Chlorobenzene derivatives are generally less reactive then their bromo counterparts.[48] In order to solve this problem, 4-bromo-aniline was replaced with 4-chloro-aniline to form the in situ boronate intermediate (Scheme 2.2 D). Using 4-chloro-aniline in the reaction gave the desired pure product, 6-(4-aminophenyl)-2*H*-chromen-2-one, in a 64% yield.

To improve the yield of this reaction different alterations were attempted as well. The presence of oxygen and water could decrease the yield of the desired product. It has been observed that in the presence of oxygen, the competing self coupling reaction of aryl boronates can be accelerated.[47] It is possible that oxygen could also contributed to formation of other side products. In addition, cross coupling reactions under aqueous conditions can lead to competitive hydrolic deboronation.[48] Therefore, the reactants were oven dried and extensively degassed before the reaction was started. The yield for this reaction was slightly decreased to 58%. This indicated that the possible presence of oxygen or water is not the problem with the reaction.

One possibility is that not enough of 4-chloro-aniline was converted to the borylated intermediate before the addition of the second base, K_2CO_3, and 6-bromo-2H-chromen-2-one, so 3 hours instead of 2 hours was given before their addition. Unfortunately the time increase allowed the aniline to couple to itself and decreased the desired product yield to 33%. Future reactions used the optimized conditions of 2 hours for the in situ borylation of 4-chloro-aniline to occur. Replacing the Suzuki and subsequent reduction reactions with a one-pot in situ Miyaura borylation followed by

Suzuki coupling reaction improved the yield of the overall synthesis of CXL070 by 20% to an overall yield of 45% (Scheme 2.3).

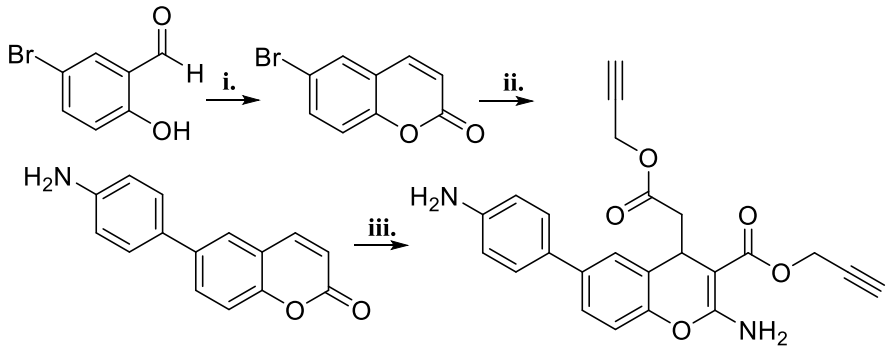

Scheme 2.3 Revised synthesis of CXL070 Reagents and conditions: (i) DMA, $POCl_3$, DCM, 0 °C to 80 °C, 4 h, $NaHCO_3$, 60 °C, 1 h; (ii) 2-chloro-aniline-4,6-d_2, XPhos Pd G2, XPhos, KOAc, $B_2(OH)_4$, EtOH, 80°C, 2h, K_2CO_3, 80°C, 18h. (iii) Ethyl cyanoacetate, Na, C_3H_3OH, rt, 24h

Using the same revised synthesis scheme reviewed above, a deuterated analog comparable to CXL070 was also synthesized, CXL D2 (Scheme 2.4). The one-pot reaction produced 6-(3,5-deuterium-2-aminophenyl)-2*H*-chromen-2-one intermediate in 74% yield. The compound was initially designed as a deuterated analog of CXL070 to be used in future biological experiments.

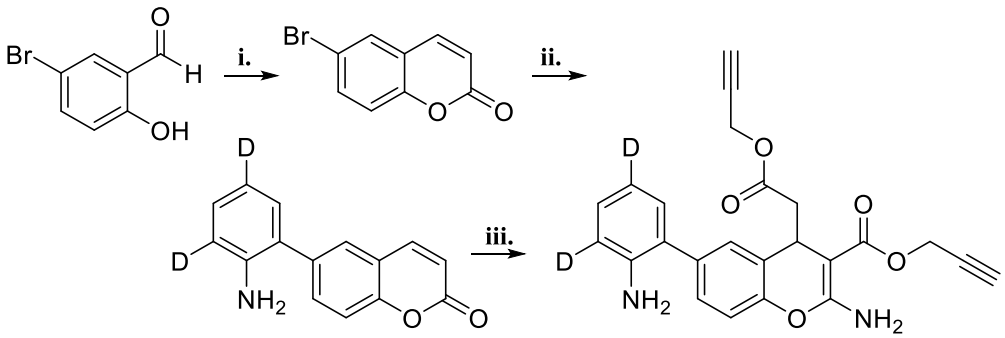

Scheme 2.4 Synthesis of deuterated CXL analog Reagents and conditions: (i) DMA, $POCl_3$, DCM, 0 °C to 80 °C, 4 h, $NaHCO_3$, 60 °C, 1 h; (ii) 2-chloro-aniline-4,6-d_2, XPhos Pd G2, XPhos, KOAc, $B_2(OH)_4$, EtOH, 80°C, 2h, K_2CO_3, 80°C, 18h. (iii) Ethyl cyanoacetate, Na, C_3H_3OH, rt, 24h.

2.2.2 In vitro cytotoxicity of deuterated CXL analog

CXL compounds have exhibited an increase in potency in cancer cells resistant to conventional therapies. The potency of the new CXL analog was determined using a well-established cell viability experiment in HL60 and mitoxantrone resistant HL60/MX2 cell lines (Figure 2.3).[26, 27, 29, 40] The most potent compound to date is CXL070, which has a reported IC_{50} value of 0.61±0.08μM in both HL60 and HL60/MX2 cells.[29] The deuterated analog exhibited IC_{50} values greater than CXL070 but more potent than CXL017, which has reported IC_{50} values of 10.7±0.5μM and 2.43±0.2μM in HL60 and HL60/MX2 cells respectively.[27] CXL D2, like most CXL compounds, was found to be more potent in resistant HL60/MX2 cells than the parental HL60 cells.

Compound	IC_{50} in HL60	IC_{50} in HL60/MX2
CXL D2	7.96 ± 1.4	2.97 ± 1.2

Figure 2.3 Cytotoxicity of CXL D2 in HL60 and HL60/MX2 cells CXL D2 was evaluated in a cell viability assay at various concentrations in HL60 and HL60/MX2 cells. The IC_{50} (μM) was determined from the fit of a dose-response curve to the four-parameter dose-response equation (Eq. 2.1). Values are an average of two independent experiments.

2.3 Conclusion

CXL070 is the most potent compound in the CXL library. In order to test the effects of CXL070 in more biological experiments including animal studies, an efficient and high yielding synthetic route must be implemented. By replacing two steps with a two step one pot cross coupling reaction in the synthetic route, the overall yield for CXL070 was improved by 20% to 45%. Using this same scheme a deuterated CXL analog was synthesized and characterized as a standard for future experiments.

2.4. Materials and methods

2.4.1. Chemistry

All commercial reagents and anhydrous solvents were purchased from vendors and were used without further purification or distillation unless otherwise stated. Analytical thin layer chromatograph was performed on Whatman silica gel 60 Å with fluorescent indicator (partisil K6F). Compounds were visualized by UV light and/or stained with iodine. Flash column chromatography was performed on Whatman silica gel 60 Å (230−400 mesh). NMR (^{1}H and ^{13}C) spectra were recorded on a Bruker 500 MHz spectrometer and calibrated using an internal reference. ESI mode mass spectra were recorded on an Agilent MSD SL ion trap. All the compounds synthesized were racemic mixtures. Purity of the compounds was analyzed by HPLC using a gradient from 10 to 95% ACN/H2O as the mobile phase with a flow rate of 1.0 mL/min over 40min on a C18 column. All final compounds exhibited greater than 95% purity and were tested in vitro as racemic mixtures.

2.4.2. General procedure for the synthesis of substituted coumarin

To *N*,*N*-dimethylacetamide (1.98 mmol) stirred at 0 °C, phosphorus oxychloride (1.98 mmol) was added dropwise. The reaction mixture was allowed to stir at 0 °C for 30 min followed by addition of the corresponding salicylaldehyde (0.99 mmol) in dry DCM. The reaction solution was then refluxed (at 60°C) for 4 h. After the allotted duration, the reaction was cooled to room temperature and saturated $NaHCO_3$ solution (10 mL) was added. The combined mixture was heated again to 60 °C for an additional 1 h, cooled, and acidified (1 N HCl). Following extraction with methylene chloride, the combined

extracts were dried (anhydrous $MgSO_4$) and concentrated under reduced pressure to afford a crude product, which upon base treatment (NaOH) followed by recrystallization gave the pure compound. If required, purification was carried out by column chromatography.

2.4.2.1. 6-bromo-2H-chromen-2-one Yield: 88%. ^{1}H NMR (500 MHz, $CDCl_3$): δ 7.62 (1H, d, J = 9.5 Hz), 7.58 (2H, m), 7.18 (1H, d, J = 8.5 Hz), 6.43 (1H, d, J = 9.5 Hz). ^{13}C NMR (100 MHz, $CDCl_3$): δ 159.93, 152.90, 142.14, 134.57, 130.19, 120.33, 118.61, 117.83, 116.97.

2.4.3. General procedure for the synthesis of 6-aryl-substituted coumarin

To halogen substituted aryl compound (0.5 mmol), potassium acetate (1.5 mmol), tetrahydroxyborane (1.5 mmol), XPhos (2 mol%), and XPhos Pd G2 (1 mol%), were added in dry ethanol, degassed, backfilled with N_2, and then stirred at 80^{o}C for two hours. To the mixture a second halogen substituted aryl compound (0.5 mmol), and potassium carbonate (1.5 mmol) were added in dry ethanol. Reaction continued for 18 hours, contents were then filtered over celite, and washed with ethyl acetate (3 X 10mL). Solvent was removed under reduced pressure to yield a crude mass, which was then extracted with ethyl acetate (3 X 10mL), and dried (Na_2SO_4). Removal of organic extracts under reduced pressure afforded the crude product, which upon column purification gave the pure product.

2.4.3.1. 6-(4-nitrophenyl)-2*H*-chromen-2-one Yield: 48%. ^{1}H NMR (500 MHz,

$CDCl_3$): δ 8.34 (2H, d, J = 8.5 Hz), 7.80−7.73 (5H, m), 7.47 (1H, d, J = 8.5 Hz), 6.52 (1H, d, J = 9.5 Hz). ^{13}C NMR (100 MHz, $CDCl_3$): δ 160.37, 154.48, 147.52, 145.83, 143.19, 135.45, 130.89, 127.93, 126.74, 124.48, 119.47, 117.95, 117.79.

2.4.3.2. 6-(4-aminophenyl)-2*H*-chromen-2-one Yield: 64%. ^1H NMR (500 MHz, $CDCl_3$): δ 7.74 (1H, d, *J* = 9.5 Hz), 7.68 (1H, dd, *J* = 2, 8.5 Hz), 7.59 (1H, s), 7.39 (2H, d, *J* = 8.5 Hz), 7.35 (1H, d, *J* = 9 Hz), 6.77 (2H, d, *J* = 8 Hz), 6.44 (1H, d, *J* = 9.5 Hz), 3.79 (2H, s). ^{13}C NMR (100 MHz, $CDCl_3$): δ 160.93, 152.78, 146.32, 143.64, 137.88, 130.12, 129.57, 127.95, 125.02, 118.99, 117.11, 116.83, 115.47.

2.4.3.3. 6-(3,5-deuterium-2-aminophenyl)-2*H*-chromen-2-one Yield: 74%. ^1H NMR (500 MHz, $CDCl_3$): δ 7.72 (1H, d, *J* = 9.5 Hz), 7.64 (1H, dd, *J* = 2, 8.5 Hz), 7.58 (1H, s), 7.40 (2H, d, *J* = 8.5 Hz), 7.19 (1H, s), 7.11 (1H, s), 6.46 (1H, d, *J* = 9.5 Hz), 3.79 (2H, s). ^{13}C NMR (100 MHz, $CDCl_3$): δ 160.70, 153.15, 143.44, 143.35, 136.01, 132.81, 130.33, 128.88, 128.22, 125.65, 119.12, 118.68, 117.33, 117.06, 115.59.

2.4.4. General procedure for the synthesis of substituted alkyl-4*H*-chromene-3-carboxylate

Freshly cut sodium (0.096 mmol) was added to propargyl alcohol (5 mL), followed by the addition ethyl cyanoacetate (0.192 mmol). The reaction mixture was stirred at room temperature under an inert atmosphere for 30 min, followed by the addition of a solution of the corresponding coumarin (0.08 mmol) in anhydrous propargyl alcohol (3 mL). The resulting reaction mixture was stirred at room temperature. Upon consumption of the

coumarin, the reaction mass was concentrated, diluted with water (30 mL), and extracted using ethyl acetate (3 × 20 mL). The organics were combined, washed with water, brine, and dried ($MgSO_4$). Removal of solvent under reduced pressure afforded the crude mass, which upon column purification gave the pure product. Note: propargyl alcohol used for this reaction must be rigorously dried.

2.4.4.1. Prop-2-yn-1-yl 2-amino-6-(3,5-deuterium-2-aminophenyl)-4-(2-oxo-2-(prop-2-yn-1- yloxy)ethyl)-4*H*-chromene-3-carboxylate (CXL D2) Yield: 67%. ^{1}H NMR (500 MHz, $CDCl_3$): δ 7.40 (1H, d, J = 2 Hz), 7.34 (3H, d, J = 8.5 Hz), 7.12 (1H, s), 7.06 (1H, s), 6.91 (2H, d, J = 8.5 Hz), 6.48 (2H, s), 4.78 (2H, t, J = 2 Hz), 4.59 (2H, t, J = 2 Hz), 4.36−4.34 (1H, m), 3.76 (2H, s), 2.77−2.61 (2H, m), 2.47 (1H, t, J = 2 Hz), 2.24 (1H, t, J = 2 Hz). ^{13}C NMR (100 MHz, $CDCl_3$): δ 170.68, 167.84, 162.24, 148.85, 143.61, 135.96, 130.30, 128.95, 128.77, 128.32, 126.52, 125.18, 116.35, 78.70, 77.55, 75.77, 74.94, 74.32, 51.86, 51.13, 43.45, 31.27. MS (ESI, positive) m/z calcd for $C_{24}H_{18}N_2O_5D_2$ $(M + H)^+$: 419.14; found: 419.1.

2.4.4.2. Prop-2-yn-1-yl 2-amino-6-(4-aminophenyl)-4-(2-oxo-2-(prop-2-yn-1-yloxy)ethyl)-4*H*-chromene-3-carboxylate (CXL070) Yield: 67%. ^{1}H NMR (500 MHz, $CDCl_3$): δ 7.40 (1H, d, J = 2 Hz), 7.34 (3H, d, J = 8.5 Hz), 6.98 (1H, d, J = 8.5 Hz), 6.73 (2H, d, J = 9 Hz), 6.43 (2H, s), 4.79 (2H, t, J = 2 Hz), 4.58 (2H, t, J = 2 Hz), 4.39−4.36 (1H, m), 3.73 (2H, s), 2.75−2.65 (2H, m), 2.47 (1H, t, J = 2 Hz), 2.28 (1H, t, J = 2 Hz). ^{13}C NMR (100 MHz, $CDCl_3$): δ 170.88, 168.07, 162.47, 148.68, 145.95, 137.97, 130.71, 127.98, 126.27, 125.97, 125.39, 116.23, 115.47, 78.87, 77.77, 76.06, 74.97, 74.37, 51.92,

51.25, 43.53, 31.32. MS (ESI, positive) m/z calcd for $C_{24}H_{20}N_2O_5$ $(M + H)^+$: 417.14; found: 417.2.

2.4.5. Cell cultures

HL60 and HL60/MX2 were purchased from ATCC. HL60/MX2 was developed from HL60 upon exposure to mitoxantrone, a topoisomerase II inhibitor. All cell lines were grown in RPMI 1640 media (ATCC) supplemented with 10% FBS and incubated at 37°C under 5% CO_2 in air.

2.4.6. Cell viability measurement

Cytotoxicity was assessed via a growth inhibition assay as reported previously.[26] Cells were plated in 96-well plates at $1x10^4$ cells/well and treated with serial dilutions of each compound in the presence of 1% DMSO. Following 48-hour incubation, relative cell viability was determined using the CellTiter-Blue cell viability assay kit (Promega, Madison, WI). Data were plotted (relative cell viability vs. log[drug]) and fit using GraphPad Prism (San Diego, CA) according to a four-parameter dose-response equation (Equation 2.1). Based on the fit, the IC_{50} of each compound was determined.

$$Y = Y_{min} + \frac{(Y_{max} - Y_{min})}{1 + 10^{n(pIC_{50} - p[X])}}$$

Equation 2.1 Four-parameter dose-response equation

Chapter 3: SERCA target characterization via photoaffinity labeling with CXL based probe compounds

3.1 Introduction

In previous experiments the Xing lab investigated the cytotoxic mechanism of action of CXL compounds. One study revealed treatment of NALM-6 and JURKAT cells with initial lead compound of the CXL series, sHA 14-1 (Figure 3.1), induced a dose-dependent increase of cytosolic calcium levels.[25] Subsequent treatment of NALM-6 and JURKAT cells with TG, a SERCA inhibitor, revealed no further increase of cytosolic calcium levels, indicating that treatment with sHA 14-1 and TG induced calcium release from the same organelle, the ER.[25] SERCA was investigated as the possible target responsible for calcium release from the ER. In an enzymatic activity assay, sHA 14-1 revealed moderate inhibition of SERCA1A and 2B, with IC_{50} values of 29.2 ± 4.9 and 23.5 ± 4.2 μM respectively.[25] Inhibition of SERCA can lead to ER stress and subsequent cell death. An increase in the expression of the ER stress-associated transcription factor ATF4 was observed in NALM-6 cells upon sHA 14-1 treatment.[25] An increase in ATF4 indicated an induction of ER stress, by sHA 14-1. Induction of ER stress, as a result of SERCA inhibition, contributed to the cytotoxicity of sHA 14-1.

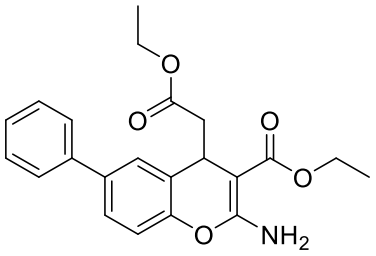

sHA 14-1

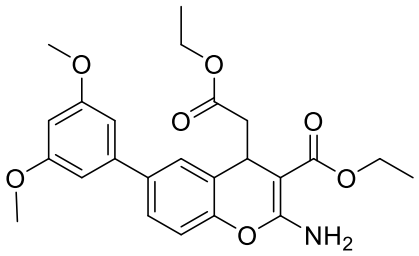

CXL017

Figure 3.1 Structures of sHA 14-1 and CXL017

To confirm the cytotoxic effect CXL compounds introduced via SERCA inhibition, a later lead compound (-)-CXL017 (Figure 3.1) was tested in a SERCA ATPase activity assay. Compound (-)-CXL017 inhibited SERCA activity, with an IC_{50} value of 13.5 ± 0.5 μM.[28] In the same activity assay, synergy in SERCA inhibition was observed when (-)-CXL017 was combined with known SERCA inhibitors TG, BHQ, and CPA, while the effect of the combinations of TG, BHQ, and CPA were simply additive in the activity assay.[28] SERCA ATPase activity assay results suggested that the conformation induced by (-)-CXL017 binding was complementary to those induced by TG, CPA, and BHQ binding in the transmembrane region of SERCA.[28] Synergy in cytotoxicity was also revealed in a cell viability assay when (-)-CXL017 and TG were dosed together in HL60 and HL60/MX2 cells.[28] The synergy observed in cytotoxicity supported the role of SERCA inhibition in the mechanism of action of (-)-CXL017 in cells. Further investigations are needed to characterize the binding site of CXL on SERCA and to identify other potential CXL targets in vitro.

Photoaffinity labeling probe-based target characterization has often been used to identify the targets and binding sites of small biologically active molecules.[49, 50] Photoaffinity probes are typically analogs of nonphotoreactive small molecules of biological interest. Probes, while photoreactive, retain the bioactivity of the small molecule, suggesting they bind to the same targets. Probes typically consist of three parts - a photoreactive group, a chemoselective scaffold, and a purification handle.[51] The photoreactive group, such as an aryl azide, is designed to form a covalent bond between the target protein and the probe upon exposure to UV light. Once exposed to UV light,

the aryl azide forms a reactive nitrene intermediate, which then reacts quickly via bond insertion, or rearrangement followed by nucelophilic attack (Scheme 3.1).[52, 53] The chemoselective scaffold is reflective of the nonphotoreactive molecule and is designed to selectively bind targets. The purification handle, such as biotin, is used to isolate covalently modified targets from unmodified targets through an affinity column.

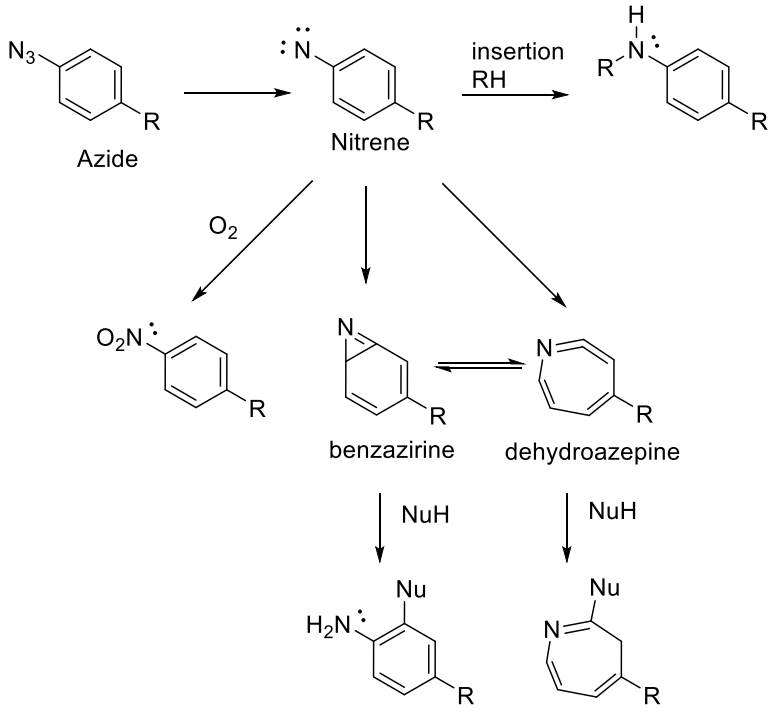

Scheme 3.1 Reactivity of aryl azides

Once the probe binds reversibly to its target, a covalent bond is formed between the probe and the target upon UV light photoactivation of the azide functional group.[50] After affinity purification, protein digestion, and LC-MS/MS analysis, the targets can be identified and/or the binding site can be predicted.[54] Experiments were completed using

photoaffinity probes CXL039, (-)-CXL037 and (+)-CXL037 respectively to determine the exact binding site of CXL compounds on SERCA, and to directly identify CXL targets in vitro.

3.2 Results and discussion

3.2.1 Characterization of CXL binding site on SERCA

In a binding competition assay with isolated SERCA1A, (-)-CXL017 revealed competition with ATP.[28] This competition suggested that CXL analogs bind to SERCA in a way that inhibits the ability of ATP to bind, resulting in SERCA inhibition. In order to confirm the mode of SERCA inhibition by CXL compounds, the exact binding site must be deduced. To investigate the CXL binding site on SERCA, two routes were carried out in parallel. One route consisted of the co-crystallization of SERCA with the cytotoxic enantiomer of CXL017, (-)-CXL017. The X-ray crystallography was completed by Dr. John Lee in the Dave Thomas group. An additional route was designed, foreseeing the difficulty of the co-crystallization of transmembrane proteins, which used tandem LC-MS/MS to detect amino acids on SERCA covalently modified upon UV exposure to a bound photoaffinity probe CXL039.[55, 56] The photoaffinity labeling protocol is illustrated in Figure 3.2 A.

A)

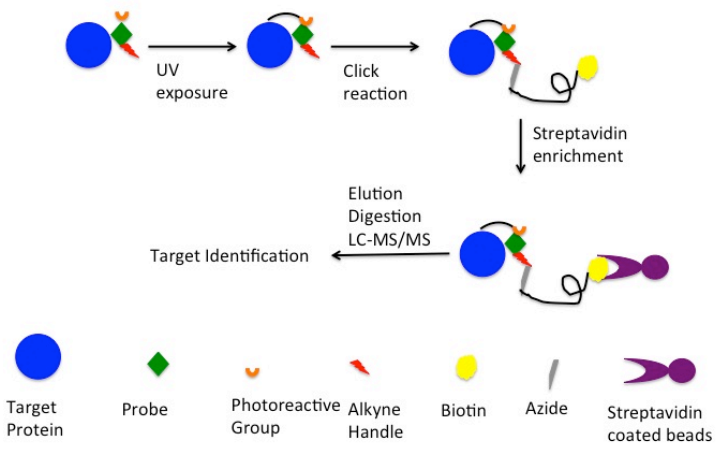

B)

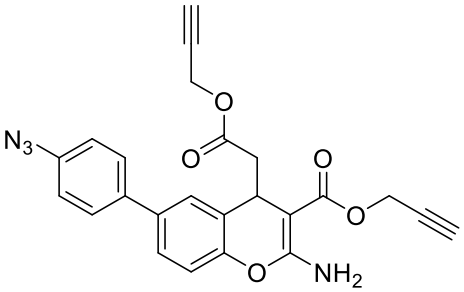

CXL039

C)

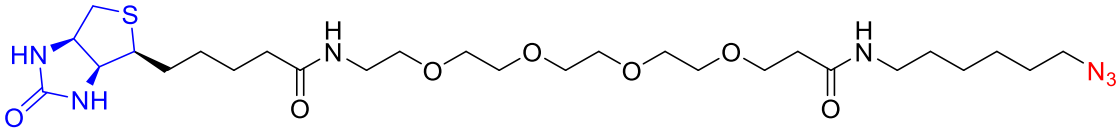

Biotin-PEG-Azide linker before the click reaction

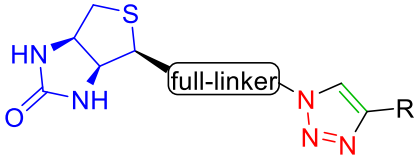

After the click reaction with alkyne

Figure 3.2 Photoaffinity labeling scheme A) The scheme of target protein labeling, enrichment, and MS identification with photoaffinity labeling probe. B) The structure of probe CXL039 C) The structure of biotin linker before and after the click reaction.

The labeling of SERCA was completed as follows. Purified SERCA1A (μM) was incubated with 5μM of CXL039 for 30 minutes in the absence of light. The mixture was then exposed to 365nm light for 10 minutes at 0°C. Exposure caused the photoreactive

aryl azide on CXL039 to react and form a covalent bond with an atom in its binding site on SERCA. A click reaction followed to attach a biotin-PEG-azide linker with the alkyne groups of CXL039. The click reaction occurred when samples were incubated for 1 hour in the absence of light with Biotin, TCEP, TBTA and $CuSO_4$ in final concentrations of 25 µM, 1mM, 250µM and 1mM respectively. Samples were then analyzed by PAGE followed by a Western blot probing with Strep-HRP for the detection of biotinylated proteins and probing with anti-SERCA antibody for the detection of SERCA. A representative Western is below containing controls that reveal CXL039 and $CuSO_4$ are both necessary for biotin visualization of SERCA (Figure 3.3). This indicated that biotin could not bind to SERCA without CXL039 and the click reagents.

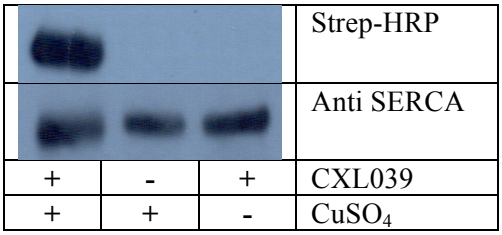

Figure 3.3 CXL039 labeling of SERCA Following 30 min incubation with or without CXL039 and exposure to 365 nm light, biotin was conjugated to the probe-protein complex via a click reaction with or without $CuSO_4$. The protein was subjected to SDS-PAGE, transferred to PVDF membrane, and visualized with a streptavidin-HRP conjugate, or anti-SERCA antibody. The chemiluminescent signal was detected by x-ray film.

In order to identify the specific peptide labeled by CXL039 via mass spectrometry, the labeled SERCA protein needed to be separated from unlabeled SERCA. Due to the strong interaction between biotin and streptavidin, magnetic streptavidin coated beads, M280, were investigated to enrich the biotinylated SERCA. After the click reaction, samples were incubated on a rotary shaker with M280 beads for one hour at 4°C for enrichment to occur. The supernatant was removed and beads were washed three times with 1M NaCl, 1%SDS, and water to remove any nonspecific proteins bound to the beads. Biotinylated samples were then eluted by incubation with 1X loading buffer at 95°C for 5 minutes. PAGE and the subsequent Western probing for biotin and SERCA in the supernatant and elution followed. A representative Western is in Figure 3.4.

	A	**B**	**C**	**D**	**E**	**F**	**G**	**H**
CXL039	+		-		+		+	
$CuSO_4$	+		+		+		-	
UV	+		+		-		+	
Supernatant	+	-	+	-	+	-	+	-
Elution	-	+	-	+	-	+	-	+
Strep-HRP								
Anti-SERCA								

Figure 3.4 Enriched CXL039 labeled SERCA Following 30 min incubation with or without CXL039 and exposure to 365 nm light, biotin was conjugated to the probe-protein complex via a click reaction with or without $CuSO_4$. The labeled proteins were then enriched using streptavidin coated M280 beads. The supernatant contains proteins that did not bind to the streptavidin coated beads and remained suspended after incubation. The elution contains proteins that were removed from the beads under elution conditions. Samples were subjected to SDS-PAGE, transferred to PVDF membrane, and

visualized with a streptavidin-HRP conjugate, or anti-SERCA antibody. The chemiluminescent signal was detected by x-ray film.

As expected, the biotin signal was only observed in the elution step when CXL039, UV exposure, and all click reagents were present (Figure 3.4 B), indicating that biotinylated SERCA was enriched. Unexpectedly, the majority of the SERCA protein was visualized in the elution steps regardless of CXL039 or UV exposure (Figure 3.4 D, F). This indicated that unlabeled SERCA was also enriched. The removal of the click reagent $CuSO_4$ exhibited a dramatic decrease in the amount of unlabeled SERCA in the elution (Figure 3.4 H). This indicated that in the presence of $CuSO_4$, SERCA would non-specifically bind to the streptavidin coated beads. This nonspecific binding was noted even after washing the beads in a variety of harsh conditions such as 6M Urea, or pre-coating the streptavidin beads with BSA. Further optimization revealed that dialysis could be used to remove the click reagents before bead enrichment; as a result the nonspecific binding of SERCA to the beads was significantly decreased (Figure 3.5 B, D).

	A	B	C	D
CXL039	+	-	+	-
Supernatant	+	+	-	-
Elution	-	-	+	+
Strep-HRP	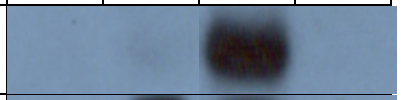			
Anti-SERCA	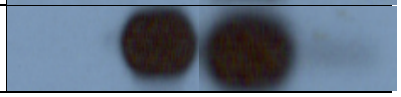			

Figure 3.5 Dialyzed enriched CXL039 labeled SERCA Following 30 min incubation with or without CXL039, biotin was conjugated to the probe-protein complex via a click reaction. The labeled proteins underwent dialysis for 48h followed by enrichment using streptavidin coated M280 beads. The supernatant contains proteins that did not bind to the streptavidin coated beads and remained suspended after incubation. The elution contains proteins that were removed from the beads under elution conditions. Samples were subjected to SDS-PAGE, transferred to PVDF membrane, and visualized with a streptavidin-HRP conjugate, or anti-SERCA antibody. The chemiluminescent signal was detected by x-ray film.

Following the optimized labeling and enrichment protocols, peptides were prepared for the mass spectrometer. Labeled SERCA was digested using trypsin. The biotinylated peptides were then enriched using M280 beads. After samples were desalted, the resulting peptides were then run through the Orbitrap Velos mass spectrometer. Results were analyzed using Proteome Discoverer to identify any SERCA peptides with the possible predicted CXL039 fragment modifications (Figure 3.6).[53] After multiple attempts, no modified peptides that were specific to SERCA labeled with CXL039 were identified. Peptides that were identified with a correct modification in the CXL039 labeled sample were also identified in the control sample that did not contain CXL039. The identification in both samples indicated that the modification was not specific to the probe. One possibility was that CXL039 was not fragmented as predicted, resulting in an unknown mass modification. Another possibility was that the labeled peptide was not enriched enough to be detected by the mass spectrometer.

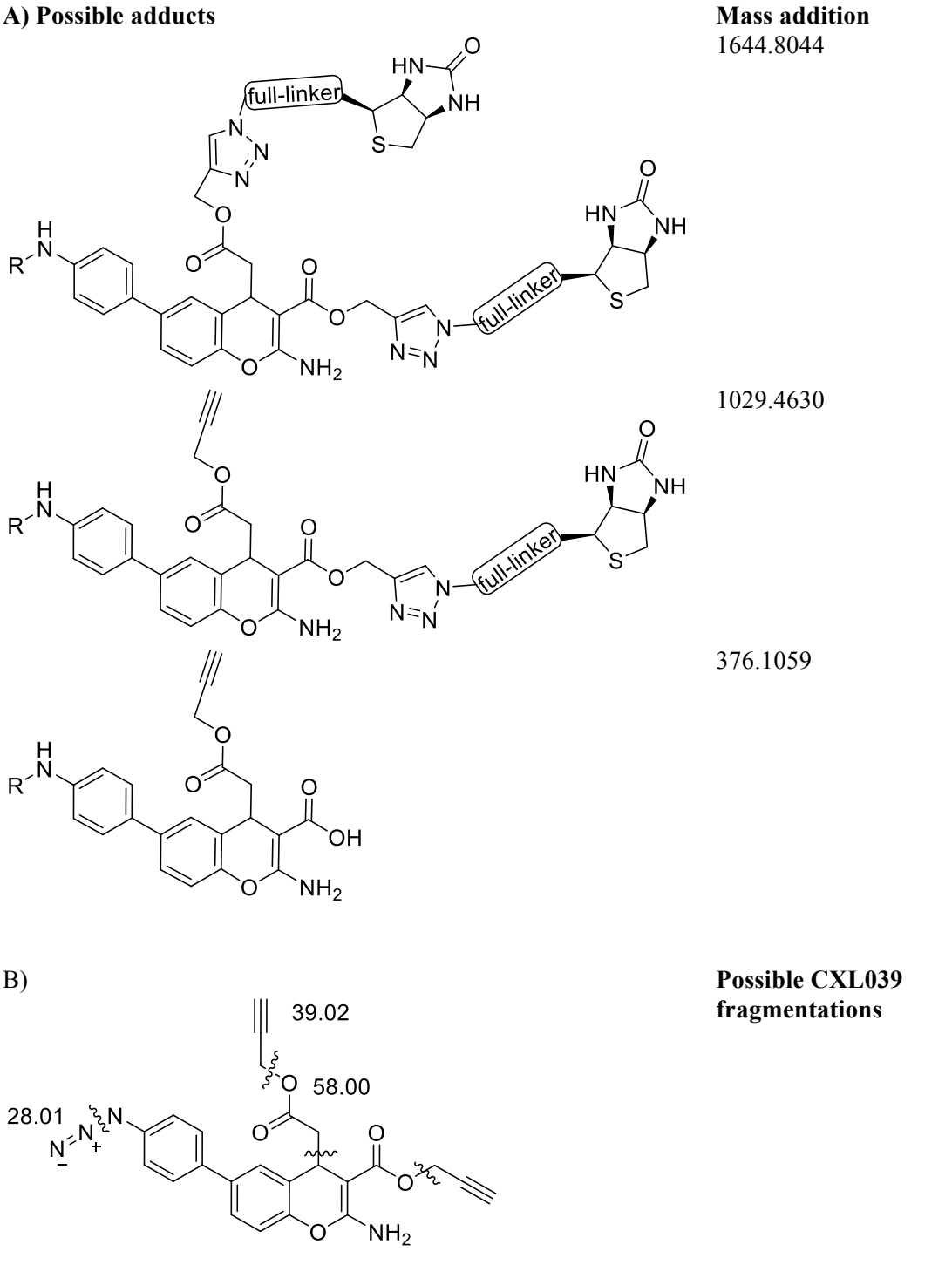

Figure 3.6 Predicted modifications A) Predicted modifications are based on nitrene insertion and a model click reaction conducted with CXL070 and click reagents. B) Possible CXL039 fragmentations monitored after UV exposure of CXL039. The

reactions were monitored by HPLC and mass spectrometry. These possible mass additions were applied to the amino acids when searching for the modified SERCA peptide in Proteome Discoverer.

Since the specific CXL039 modification could not be detected, indirect evidence of the SERCA peptide labeled with CXL039 was investigated. Due to the unnatural modification of CXL039 the SERCA peptide labeled with CXL039 should have a relatively low abundance compared to the other unlabeled SERCA peptides. SERCA that went through the previously outlined labeling and enrichment protocol was run on PAGE, and then stained with Coomassie blue (Figure 3.7).

A	B	
		Coomassie Stain
+	-	CXL039
+	+	SERCA

Figure 3.7 Coomassie stained SERCA labeled with CXL039 Samples A and B have gone through the previously outlined labeling, dialysis and enrichment protocol with or without CXL039. PAGE was performed followed by Coomassie staining.

The corresponding bands were excised, and in gel digestion was performed. Samples were then desalted and analyzed by the Orbitrap Velos for LC-MS/MS. Analysis with Proteome Discoverer revealed an average coverage of 35% of SERCA1A sequence in both samples. There were no significant differences in the peptide abundance between

samples. This revealed that either that the labeled peptide was not covered in the 35% identified by the software, or that the relative abundance of the labeled peptide was too low to detect a difference between samples. From these experiments, no conclusions could be made about the binding site of CXL039 on SERCA. This route was no longer investigated after Dr. John Lee solved the co-crystal structure of SERCA with (-)-CXL017. The labeling conditions optimized were used in further experiments.

3.2.2 In vitro photoaffinity labeling with CXL037 enantiomers

SERCA is one putative target of CXL compounds, which remains to be validated in cells. At the same time, there might be other direct cellular targets of CXL compounds. To investigate these, a labeling experiment was designed using enantiomers of the photoaffinity probe CXL037.[55] The cellular IC_{50} values of the CXL037 enantiomers were determined using a cell viability assay in HL60 and HL60/MX2 cell lines. The (-)-CXL037 enantiomer proved to be on average 10 times more cytotoxic than (+)-CXL037 in both cell lines (Figure 3.8). These results agree with those obtained from the previous cell viability testing of (-)-CXL017, which was 13 times more cytotoxic in HL60 and 10 times more cytotoxic in HL60/MX2 than (+)-CXL017.[28]

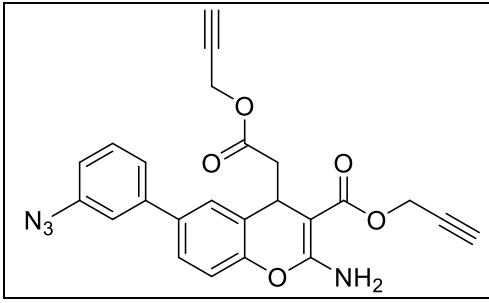

Compound	IC_{50} in HL60	IC_{50} in HL60/MX
(+/-)-CXL037	6.66 ± 1.3	3.85 ± 1.1
(+)-CXL037	42.0 ± 3.9	30.7 ± 8.9
(-)-CXL037	4.75 ± 0.87	2.55 ± 0.64

Figure 3.8 Structure and cytotoxicity of CXL037 in HL60 and HL60/MX2 cells
CXLs were evaluated in a cell viability assay at various concentrations in HL60 and HL60/MX2 cells. The IC_{50} (μM) was determined from the fit of a dose-response curve to the four-parameter dose-response equation (Eq. 2.1). Values are an average of three independent experiments.

Since (-)-CXL037 is the enantiomer responsible for the majority of the cytotoxicity of CXL037, it was used to investigate the cellular targets responsible for the cytotoxicity of CXL compounds. (+)-CXL037 was used as a control compound in these experiments due to its similar structure and relative weak of cytotoxicity. As CXL compounds tend to be more cytotoxic in HL60/MX2 cells than in their parental HL60 cells, HL60/MX2 cells were used in for the in vitro labeling experiment to identify the targets of CXL compounds responsible for cytotoxicity.[27, 29] Conditions that could affect the labeling profile were investigated, including incubation time, drug concentration, and purification conditions.[57]

All in vitro labeling experiments were conducted as followed unless otherwise stated. All compounds were incubated with HL60/MX2 cells at the indicated

concentrations for the indicated time. Cells were then exposed to 312nm UV light for 10 min. Cells were then washed with PBS and lysed using RIPA buffer and intermittent sonication. The solution was then centrifuged at 17.0 times gravity and the supernatant was then collected and analyzed for protein concentration using a BCA assay. The protein concentration was then normalized to 1μg/μL. After normalization, the click reaction was conducted to attach a biotin-azide linker to the alkyne handles of CXL037 (Figure 3.8). The reaction occurred as follows: 270pmol of protein was incubated with biotin, TCEP, TBTA and $CuSO_4$ in final concentrations of 25μM, 1mM, 250μM and 1mM respectively. PAGE and subsequent Western for biotin detection followed.

To optimize the incubation time needed for effective protein labeling, HL60/MX2 cells were incubated with 5μM of (+)-CXL037, (-)-CXL037, or DMSO for 30 minutes, 1.5 hours, or 3 hours before exposure to 365nm for 10min. The rest of the experiment was carried out as indicated (Figure 3.9).

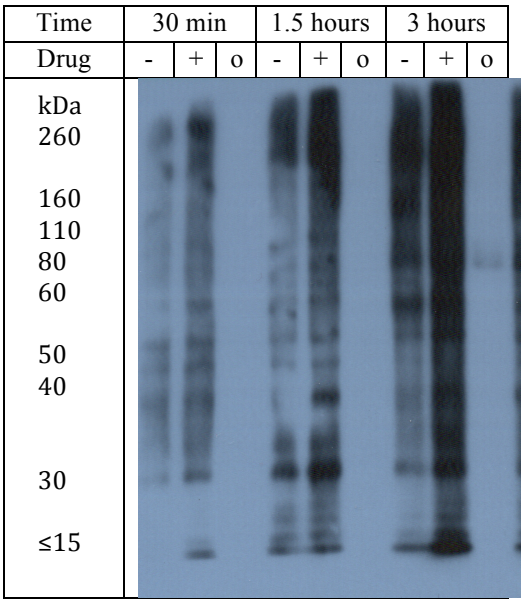

Figure 3.9 Effect of incubation time on CXL037 labeling Intact HL60/MX2 cell-based photoaffinity labeling of the cellular target proteins via the cytotoxic (-)-CXL037 and non-cytotoxic (+)-CXL037 photoaffinity probes. For the indicated time, cells were incubated with or without (o) the indicated CXL037 enantiomer (-, +) at 5μM. Cells were exposed to 312 nm light, then lysed and normalized for protein concentration. Biotin was conjugated to the probe-protein complexes via a click reaction. Samples were subjected to SDS-PAGE, transferred to PVDF membrane, and visualized with a streptavidin-HRP conjugate. The chemiluminescent signal was detected by x-ray film.

The labeling of HL60/MX2 cells was observed to be time dependent. As expected, the longer the compounds were incubated with the cells, the more proteins were labeled. Unexpectedly, the same proteins that were labeled with (-)-CXL037 were also labeled with the relatively noncytotoxic (+)-CXL037 in higher abundance. This could be a result of incubation with too high of a concentration of compound resulting in nonspecific

protein labeling. Since the best time of proteins labeled by the cytotoxic compound (-)-CXL037 was at 3 hours, this time point was used in future experiments.

In order to determine whether changing the concentration of CXL037 would have an effect on the difference of labeling between enantiomers, the labeling experiment previously outlined was carried out using varying concentrations. HL60/MX2 cells were incubated with 5μM, 2.5μM, 1.25μM, .625μM, .3125μM, or 0μM of (+)-CXL037 or (-)-CXL037 for 3 hours before exposure to 365nm for 10min. The rest of the experiment was carried out as indicated (Figure 3.10).

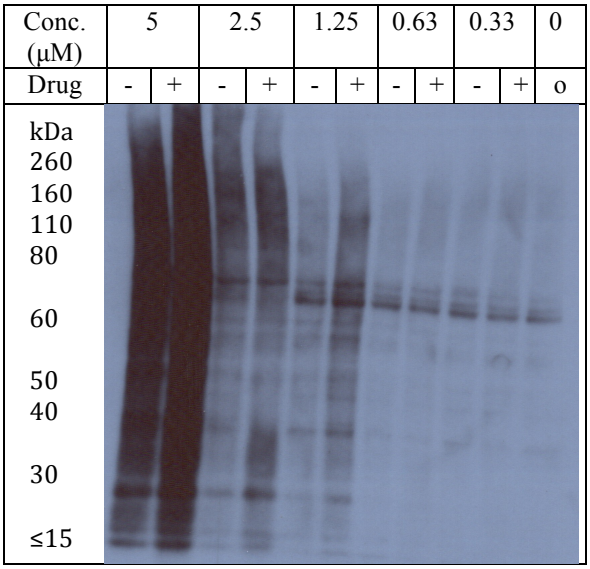

Figure 3.10 Effect of CXL037 concentration on protein labeling in HL60/MX2 Intact HL60/MX2 cell-based photoaffinity labeling of the cellular target proteins via the cytotoxic (-)-CXL037 and non-cytotoxic (+)-CXL037 photoaffinity probes. For 3 hour cells were incubated with or without (o) the indicated CXL037 enantiomer (-, +) at the specified concentration. Cells were exposured to 312 nm light, then lysed and normalized

for protein concentration. Biotin was conjugated to the probe-protein complexes via a click reaction. Samples were subjected to SDS-PAGE, transferred to PVDF membrane, and visualized with a streptavidin-HRP conjugate. The chemiluminescent signal was detected by x-ray film.

As expected, the same proteins were labeled at all of the varying concentrations of CXL037, but the amount of these proteins increased as the concentration of CXL037 increased. It should be noted that the lower the concentration the longer the exposure time was needed to visualize the proteins. The same proteins that were labeled with (-)-CXL037 were also labeled with (+)-CXL037 in higher abundance. The results revealed a minimal difference between the lower doses 0.625μM, 0.3125μM, and the DMSO control, suggesting that the bands visible are not specific to the drug treatment. The lowest concentration with a visible difference between cells treated with CXL037 enantiomers and DMSO is 1.25μM. In future experiments, 1.25μM was used. It was possible that the streptavidin-HRP is unspecifically labeling bands in the lysate.[57] In order to reduce the intensity of these nonspecific bands, the enrichment protocol previously outlined with streptavidin coated beads M280 was applied.

HL60/MX2 cells were incubated with 1.25μM or 0μM of CXL037 enantiomers for 3hours. After UV exposure, cell lysis, protein quantification, and click reaction samples were incubated with M280 beads for 1hour at 4°C on a rotary shaker. Samples were then washed and eluted from the beads as previously described. PAGE was then performed on the eluted samples, followed by Western analysis with streptavidin-HRP

(Figure 3.11 A). Since the target proteins may only be weakly labeled by CXL037 compounds, the Western blot was also probed for some known proteins affected by CXL compounds, SERCA, Mcl-1, and Bcl-2 (Figure 3.11 B).[25, 26, 40]

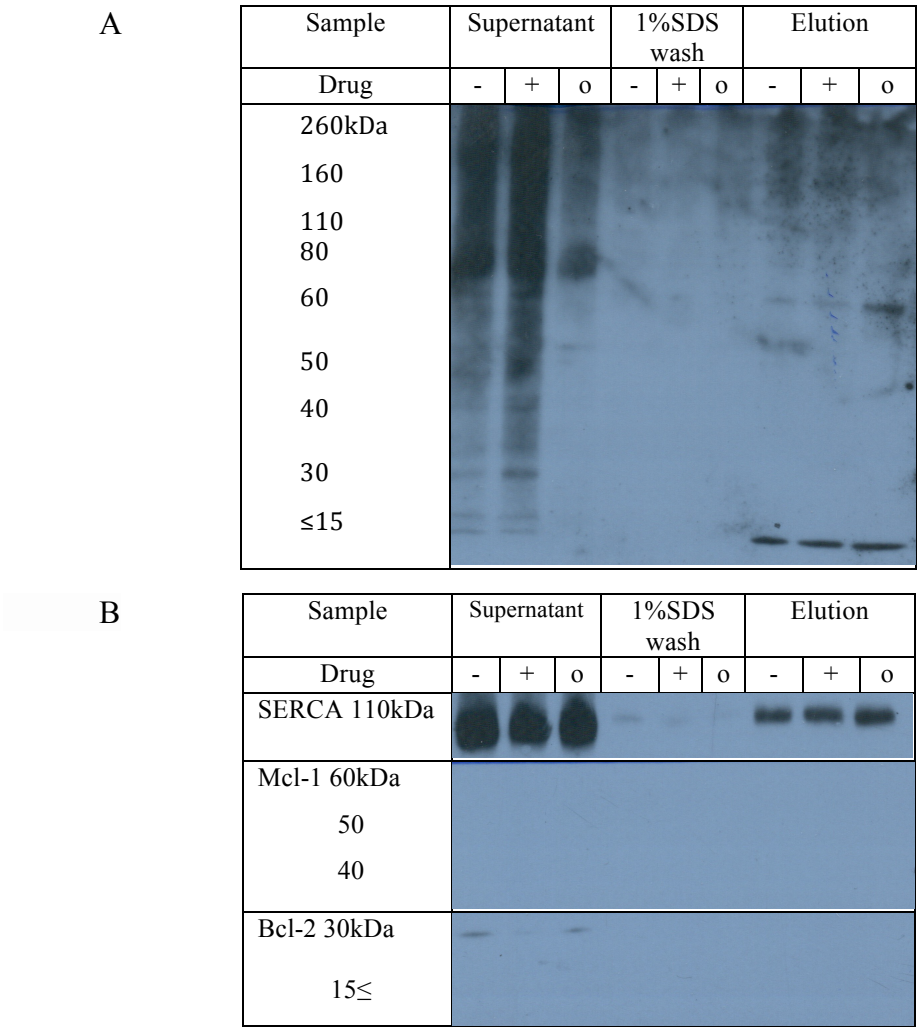

Figure 3.11 Enrichment of CXL037 labeled proteins Intact HL60/MX2 cell-based photoaffinity labeling of the cellular target proteins via the cytotoxic (-)-CXL037 and non-cytotoxic (+)-CXL037 photoaffinity probes. For 3 hour cells were incubated with or without (o) the indicated CXL037 enantiomer (-, +) at 1.25μM. Cells were exposed to

312 nm light, then lysed and normalized for protein concentration. Biotin was conjugated to the probe-protein complexes via a 'Click' reaction. The labeled proteins were then enriched using streptavidin coated M280 beads. The supernatant contains proteins that did not bind to the streptavidin coated beads and remained suspended after enrichment. The 1%SDS wash lanes contained proteins that were removed from the beads by washing with 1%SDS. The elution contained proteins that were removed from the beads under elution conditions. Samples were subjected to SDS-PAGE, transferred to PVDF membrane, and visualized with a streptavidin-HRP conjugate or the specified antibody. The chemiluminescent signal was detected by x-ray film.

Bands visible on the film in the supernatant lanes of Figure 3.11 A are visible due to either a nonspecific interaction with the Streptavidin-HRP, or not enough time was given for the proteins to bind to the beads. No band specific to labeling with CXL037 was visible in the elution of Figure 3.11 A. No signal was observed when the membrane was probed for Mcl-1. Bcl-2 was seen in the supernatant lanes of Figure 3.11 B, but this signal was not observed in the elution. This indicated that Mcl-1 and Bcl-2 were not labeled by CXL037. When the membrane was probed for SERCA, the majority of signal was observed in the supernatant lanes with less intense bands visible in the elution lanes of all three treatments. This indicated that SERCA does not preferentially bind to the M280 beads. The intensity of the bands in the elution lanes did not differ between CXL037 treatments. This indicated their enrichment was not due to any interaction with CXL037. In previous experiments SERCA unspecifically bound to M280 beads in the presence of $CuSO_4$ used in the click reaction. This could explain its presence in the elution lanes of Figure 3.7 B. Due to no visual discrepancies between the cytotoxic

enantiomer (-)-CXL037 and the relatively noncytotoxic enantiomer (+)-CXL037, further optimization is needed before protein identification via mass spectrometry. One possibility was that the target proteins were of too low abundance to be successfully visualized by Western analysis. Another possibility was the aryl azide was too reactive of a photoaffinity probe and unselectively binds to nontargets.[58]

3.3 Conclusion

One known target of CXL compounds responsible for their cytotoxicity is SERCA. CXL photoaffinity probes, CXL039 and CXL037, were investigated for their ability to covalently label SERCA and other potential cellular targets respectively. Optimization of labeling and purification conditions remains incomplete. Future experiments include exploring other reactive photoaffinity probes, and the incorporation of isotopes into the structure of photoaffinity CXL probes to identify mass difference via mass spectrometry.

3.4 Materials and methods

3.4.1 Chemistry

CXL photoaffinity probes CXL037 and CXL039 were synthesized by Dr. Balasubramanian Srinivasan and Dr. Aridoss Gopalakrishnan based on an established protocol with CXL055 and CXL070 as precursors respectively.[59] All commercial reagents and anhydrous solvents were purchased from vendors and were used without further purification or distillation unless otherwise stated.

3.4.2 Reagents

Biotin Azide (PEG4 carboxamide-6-azidohexanyl biotin) and Imperial® Stain (Coomassie) were purchased from Life Technologies (Carlsbad, CA). Ultrasensitive streptavidin−peroxidase polymer was purchased from Sigma-Aldrich (St. Louis, MO). Lastly, SuperSignal West Pico Chemiluminescent Substrate was supplied by Thermo Fisher (Rockford, IL). Proteins for evaluation of probe specificity were provided or purchased from the following sources: BSA (Sigma-Aldrich), SERCA (Dave Thomas Group, University of Minnesota). Other reagents including triton X-100, octaethylene glycol mono-n-1-dodecyl ether (C12E8), adenosine 5′-triphosphate (ATP) disodium salt hydrate, tris-(2-carboxyethyl)phosphine (TCEP), copper sulfate ($CuSO_4$), and tris-(benzyltriazolylmethyl)amine (TBTA) purchased from Sigma-Aldrich (St. Louis, MO). The reagents and equipment for SDS-PAGE included NuPAGE Novex 4-12% Bis-Tris precast polyacrylamide gels, 4X loading buffer, NuPAGE MOPS Running Buffer, and NuPAGE Transfer Buffer and were purchased from Life Technologies (Carlsbad, CA). 1,2-dioleoyl-sn-glycero-3-phosphocholine (DOPC), 1,2-dioleoyl-sn-glycero-3-

ethylphosphocholine chloride salt (EDOPC), and 1,2-dioleoyl-sn-glycero-3-phosphoethanolamine (DOPE) were purchased from Avanti Polar Lipids. Bio-Beads SM-2 nonpolar polystyrene adsorbents were purchased from Bio-Rad. Fluorescent probes, fluorescein 5'-isothiocyanate (FITC), Fluo-5f (cell impermeant form), and 1,2-dihexadecanoyl-sn-glycero-3-phosphoethanolamine, triethylammonium salt (Texas Red) were purchased from Molecular Probes. All other reagents were of analytical grade. The original design and synthesis of CXL photoaffinity probes, CXL039 and CXL037, were carried out by Dr. Balasubramanian and Dr. Aridoss Gopalakrishnan. Initial conditions for SERCA labeling, peptide enrichment and mass spectrometry conditions were optimized by Nick Bleeker and Dr. Yuesheng Dong.

3.4.3 Purification of SERCA protein (performed by members of the Thomas lab)

SERCA was purified from skeletal muscle of New Zealand white rabbits in 0.01% $C_{12}E_8$ by the Reactive-Red method and then flash-frozen and stored in liquid nitrogen after addition of 0.5 mg of lipid (sonicated DOPC and DOPE, 4:1 ratio by weight) /mg of protein.[56, 60] Protein concentrations were determined by the bicinchoninic acid assay (BCA), using bovine serum albumin as the standard.

3.4.4 General protocol for photolabeling of purified SERCA protein

Photolabeling experiments were performed in individual wells of a 96-well pointed-bottom plate. First, protein was taken in reaction buffer (5 mM $MgCl_2$, 100 mM KCl, 1 mM EGTA, and 50 mM MOPS at pH 7.0) at a concentration of 1 μM (M.W. 100 kDa) and allowed to incubate at room temperature for 30 min with probe molecules in the

presence of 10% DMSO. Next, the plate was cooled to 0°C and samples were subjected to 365 nm light from a handheld lamp for 10 min. The lamp was placed directly atop the 96-well plate with samples centered in the path of light. Following UV irradiation, 'Click' reagents were added in the following order to yield the final indicated concentrations: Biotin-N_3 (25 μM), TCEP (1 mM), TBTA (250 μM), $CuSO_4$ (1 mM). Samples were subsequently incubated in the plate for an additional hour. After the incubation period, samples for SDS-PAGE (reducing conditions) were prepared from aliquots of the individual reaction mixtures.

3.4.5 PAGE and western analysis

Gel electrophoresis was performed at 150 V for 1.5 hours. In certain experiments, total protein was stained in-gel with Coomassie following the manufacturer's protocol. In most cases, however, transfer of protein from the gel to PVDF membrane was performed at 40 V for 3 h. The membrane was blocked with 1% BSA in PBST (PBS with 0.05% TWEEN20) and incubated with ultra-sensitive streptavidin-peroxidase polymer for 1 h at room temperature. Prior to use, the streptavidin conjugate was diluted 1:10000 in PBST. Finally, biotinylated protein was visualized upon addition of a chemiluminescent peroxidase substrate. Resultant luminescence was captured using x-ray film.

3.4.6 Cell cultures

All cell lines were grown in RPMI 1640 media (ATCC) supplemented with 10% FBS and incubated at 37 °C under 5% CO_2 in air. Detailed information regarding the original source of HL60/MX2 as well as the corresponding parental cell lines was described

previously (see Section 2.4.5).

3.4.7 Cell viability measurement

Cytotoxicity was assessed by way of the CellTiter-Blue cell viability assay kit (Promega, Madison, WI) (see Section 2.4.6).[26] Similarly data were plotted and fit (Equation 2.1) to obtain the IC_{50} of each inhibitor.

3.4.8 In vitro affinity labeling

Cells were aliquoted in 6-well plates (2×10^5 cells/well) or 10 mm petri dishes (2×10^6 cells/plate). Then compound-containing media was added at the specified concentration and were incubated for the desired time. After treatment, plates were put on a UV illuminator (312 nm) for 10 min for photo-activated labeling. Cells were then removed from the plate, washed with cold PBS and lysed with EDTA-free RIPA buffer with intermittent sonication. Protein concentration was measured with BCA kit and lysates were diluted to 1 ug/uL with PBS. To 30 uL of lysate sample was added 3 uL of each click reagents in the following order: Biotin-N_3 (25 μM, unless otherwise noted), TCEP (1 mM), TBTA (250 μM), $CuSO_4$ (1 mM). Reaction was allowed to occur for 1 hour at room temperature in the dark.

3.4.9 Affinity purification of biotinylated proteins with streptavidin beads

Dynabeads® M-280 Streptavidin bead slurry (50 μL) was taken into a microcentrifuge tube and washed thoroughly with PBS using a magnet, and then labeled protein sample was added to the washed beads. The tube was shaken with a rotary shaker at 4°C for

1hour. The beads were washed with 1M NaCl three times, 1% SDS three times, water three times, and then boiled with 14 µL of 1X loading buffer to elute the biotinylated proteins off of the beads. The elute sample was then subjected to PAGE followed by Western analysis.

3.4.10 In-gel digestion and MS identification

PAGE analysis was performed as described above, and the gel was stained with Imperial® staining to visualize the target protein band. The band was cut out and diced into 1 mm cubes. To each diced gel sample was added 100 µL 25 mM NH_4HCO_3 and 10 µL 300 mM DTT, incubated for 15 min at 50°C, and then added 10 µL saturated iodoacetamide and incubated for 15 min at RT. The resulting liquid was discarded and the gel pieces was washed twice with 1:1 ACN: 25mM NH_4HCO_3 and once with ACN. After drying with speed-vac, the gel pieces was re-suspended in 75 µL 25mM NH_4HCO_3 and 25 µL of trypsin at 0.1 µg/µL was added and the digestion was performed at 37°C for overnight. The digest was saved and combined with two peptide extractions from gel pieces with 0.1% HCOOH in 60% ACN/25 mM NH_4HCO_3. The combined digest sample was dried with speed-vac and then desalted with $ZipTip_{C18}$ column (Millipore) following manufacturer's instruction. The final desalted samples were analyzed with Thermo Orbitrap Velos LC-MS system on a C18 reverse-phase column. 5 µL of desalted sample was injected into the column and eluted with an ACN/H_2O gradient from 2% to 35% within 1 hour. Mass peaks were detected with the hi-res Orbitrap detector. The raw data thus collected was analyzed with Proteome Discoverer to identify protein hits. Quantitative study was done by extracting peaks of identified peptide hits from the TIC

of the whole sample with Thermo Qual Browser.

Chapter 4: Screening for a new chemotherapeutic scaffold

4.1 Introduction

Currently CXL compounds and their mechanism of action remain under investigation in the Xing lab. Additionally, efforts have been made to identify new drug scaffolds. One common strategy used to identify new anticancer drug templates is unbiased screening, which can be classified into biochemical based or cell-based screening assays.[61-63] Cell-based screening provides a more biologically relevant environment than isolated biochemical based screening.[64] Cell-based screening has been used to identify Ro 91-1311, Ro 23-6538, 4-aryl-4*H*-chromene compounds, and paclitaxel. The Roche Research Center identified Ro 91-1311 and Ro 23-6538 as novel antiproliferative compounds from a cell-based screen of 5000 compounds in prostate (DU145), breast (MDA435), and colon (RKO, SW480) cancer cells.[62] Maxim Pharmaceuticals Inc. identified 4-aryl-4*H*-chromene compounds, from screening a commercial compound library, as inducers of apoptosis in leukemia (HL60) and breast cancer (T47D) cells.[65] The National Cancer Institute (NCI) discovered paclitaxel from a cell-based screen of 35,000 natural products in the mouse leukemia cell lines L1210 and P388.[66] Since its discovery, paclitaxel has been widely used to successfully treat breast, prostate and ovarian cancers. Paclitaxel is just one of many chemotherapeutics isolated from natural products.

Natural products, from plants, microorganisms, and marine wildlife, have proven to be a rich source of anticancer drugs.[67] About 50% of the current chemotherapeutics are comprised of natural products or their analogs.[66] A large part of the activity of natural

products is due to their unique scaffolds and degree of stereochemistry.[67] Examples include vinca alkaloids, podophyllins, and epothilones. Vinca alkaloids such as vinblastine and vincristine are isolated from *Catharanthus roseus*. Vinblastine and vincristine have been used to treat cancers such as leukemia, testicular teratoma, and Hodgkin's disease.[68] Podophyllins, such as etoposide, were isolated from *Podophyllum peltatum,* and have been used to treat small-cell lung cancer and testicular teratoma.[68] Epothilones isolated from the mycobacterium *Sorangium cellulosum* have been approved to treat breast and ovarian cancers.[67] New natural products are continuously isolated and evaluated for their effects on cancer cells.[64]

The Xing lab used a cell viability based assay (drug sensitive and drug resistant cancer cells) to screen a library of plant-based natural products isolated from different unique species in Australia. Evaluating compounds based on their cell viability eliminates potential bias against cellular targets or mechanisms of action.[61] Compounds were evaluated for their ability to decrease cell viability in HL60 and HL60 doxorubicin resistant (HL60/DOX) leukemic strains. Several compounds were identified from these cell viability based screens that exhibited submicromolar IC_{50} values in both cell lines and unique cytotoxicity profiles.

4.2 Results and discussion

In this study our collaborator in Australia provided the Xing lab with 384 plant-based natural products. These 384 compounds were screened for their ability to inhibit cellular growth in HL60 and HL60 doxorubicin resistant cells (HL60/DOX). The

sensitivity of these cell line to DOX was verified in parallel while experiments were completed. The 384 compounds went through three rounds of screening to discover interesting lead candidates.

4.2.1 Initial screen

Initially, all compounds were tested for their ability to decrease cell viability at a single dose of 20μM in both HL60 and HL60/DOX cell lines with triplicate technical repeats. Compounds were categorized based on these results (Figure 4.1 and Figure 4.2). Compounds that revealed a cell viability measurement greater than 50% of the control at 20μM in both cell lines were excluded from further testing, due to their lack of potency. Compounds that revealed a cell viability measurement less than 50% at 20μM in either HL60 or HL60/DOX cells were subcategorized for further testing. The three subcategories were: compounds that reduced cells viability measurements in HL60 cells greater than that in HL60/DOX cells, compounds that reduced cells viability in HL60/DOX cells greater than that in HL60 cells, and compounds that effectively reduced cells viability in both cell lines. It was found that cell viability results were not dependent on the compound's placement in the 384 well plate (Figure 4.1). This initial screening identified 59 compounds that fit into these three subcategories. These 59 compounds were further tested to obtain an IC_{50} value in HL60 and HL60/DOX cell lines.

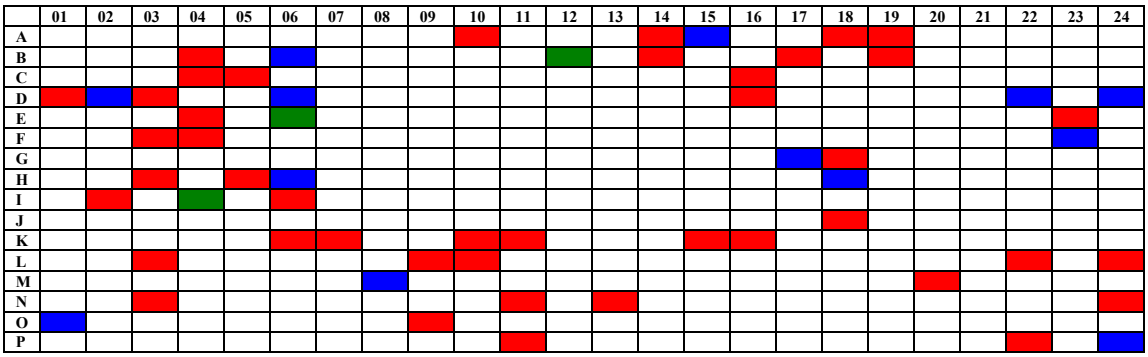

Figure 4.1 Results of the initial 20µM screen Compounds that reduced cells viability in HL60 cells greater than in HL60/DOX cells are depicted in green. Compounds that reduced cells viability in HL60/DOX cells greater than HL60 cells are depicted in blue. Compounds that effectively reduced cells viability in both cell lines are depicted in red. Compounds that revealed cell viability measurements greater than 50% in both cell lines are depicted in white.

A	Compound	HL60	HL60/DOX	B	Compound	HL60	HL60/DOX
	1B12	1.39 ± 0.6	51.8 ± 0.8		1O01	76.5 ± 4	6.82 ± 0.3
	1I04	13.6 ± 3	63.5 ± 7		1M08	81.8 ± 14	7.27 ± 1
	1E06	25.0 ± 1	67.6 ± 11		1A15	52.3 ± 6	8.17 ± 0.8
					1D02	93.2 ± 2	9.13 ± 0.8
					1D24	57.1 ± 1	10.7 ± 0.1
					1B06	114 ± 2	17.4 ± 3
					1H18	59.4 ± 2	18.0 ± 5
					1D06	102 ± 4	18.2 ± 2
					1P24	58.9 ± 3	22.2 ± 0.8
					1G17	176 ± 3	25.5 ± 3
					1F23	74.4 ± 10	25.7 ± 2
					1H06	70.9 ± 3	29.1 ± 4
					1D22	91.0 ± 5	29.9 ± 3
C	1F04	8.24 ± 0.3	40.0 ± 12		1L03	5.18 ± 1	0.564 ± 8
	1G18	6.05 ± 1	37.4 ± 10		1K10	5.08 ± 0.6	0.0107 ± 8
	1N13	1.68 ± 0.2	15.8 ± 8		1B19	19.4 ± 0.6	14.1 ± 8
	1N24	13.5 ± 0.6	26.8 ± 8		1A14	8.77 ± 0.4	3.02 ± 8
	1P22	7.91 ± 0.8	18.4 ± 7		1K06	8.12 ± 3	0.925 ± 8
	1K07	9.26 ± 0.2	17.9 ± 6		1D03	13.7 ± 0.3	6.16 ± 8
	1P11	1.62 ± 4	5.53 ± 6		1K15	10.8 ± 0.8	3.19 ± 8
	1D16	8.68 ± 2	14.9 ± 6		1C16	9.56 ± 0.9	1.08 ± 8
	1L09	6.12 ± 0.3	11.5 ± 5		1L10	23.3 ± 0.8	14.7 ± 8
	1F03	5.40 ± 1	9.15 ± 5		1B04	14.6 ± 0.4	1.42 ± 9
	1N11	4.72 ± 0.7	8.31 ± 5		1B17	15.4 ± 3	0.492 ± 9
	1I02	13.0 ± 2	16.5 ± 5		1B14	26.9 ± 3	11.6 ± 9
	1D01	3.75 ± 0.7	7.07 ± 5		1H05	18.6 ± 0.3	1.84 ± 9
	1H03	5.81 ± 2	8.63 ± 5		1L22	21.0 ± 2	3.56 ± 9
	1K11	1.30 ± 0.5	1.96 ± 4		1I06	32.1 ± 1	13.4 ± 9
	1A10	9.11 ± 0.9	8.21 ± 5		1A18	32.1 ± 0.7	12.7 ± 9
	1O09	4.10 ± 0.2	3.17 ± 5		1J18	33.5 ± 1	14.0 ± 10
	1C04	1.78 ± 0.5	0.791 ± 5		1C05	46.5 ± 9	23.7 ± 11
	1N03	10.7 ± 0.6	7.86 ± 6		1E23	38.9 ± 4	14.3 ± 6
	1L24	4.10 ± 0.6	1.06 ± 6		1A19	30.8 ± 0.4	4.32 ± 3
	1E04	8.04 ± 0.7	4.18 ± 6		1M20	27.7 ± 0.9	0.222 ± 3
	1K16	5.89 ± 0.2	1.49 ± 8				

Figure 4.2 Select average cell viability percentages obtained from 20μM dose A) Compounds with cell viability percentages less than 26% in HL60 cells B) Compounds with cell viability percentages less than 30% in HL60/DOX cells C) Compounds with cell viability percentages less than 40% in both cell lines. Compounds revealed cell

viability measurements greater than 50% in both cell lines are not reported. Values are an average of technical triplicates.

4.2.2 Second screen

To further assess their potency, the 59 compounds selected from the initial screen were evaluated at three concentrations in a HL60 and HL60/DOX cells. Their effect on cell viability was measured in triplicate technical repeats using a three-fold dilution curve starting at 20μM. Results from this screen are depicted in Figure 4.3 and 4.4. This study identified 37 compounds that estimated a double-digit micromolar IC_{50} value in both cell lines. These 37 were not further tested due to the weak potency.[69] Among the other 22 compounds, four compounds predicted IC_{50} values in HL60 cells greater than HL60/DOX cells, three compounds predicted IC_{50} values in HL60/DOX cells greater than HL60 cells, and two compounds predicted IC_{50} values equally potent in both cell lines. Additionally, 13 compounds, 1D02, 1D03, 1H03, 1E04, 1K06, 1L09, 1A10, 1N11, 1C16, 1A18, 1J18, 1A19, and 1L22, were too potent in both cell lines to reveal an accurate dose response curve. Without a dose response curve to fit to equation 2.1, an accurate IC_{50} value could not be calculated. The compounds with IC_{50} values in low micromolar or nanomolar concentrations were selected for further testing. The compounds, such as 1F03, that exhibited a preference for inhibiting cell viability in either HL60 or HL60/DOX cells were also designated for further testing. These 22 compounds were selected to determine the compound's full dose response to obtain accurate IC_{50} values.

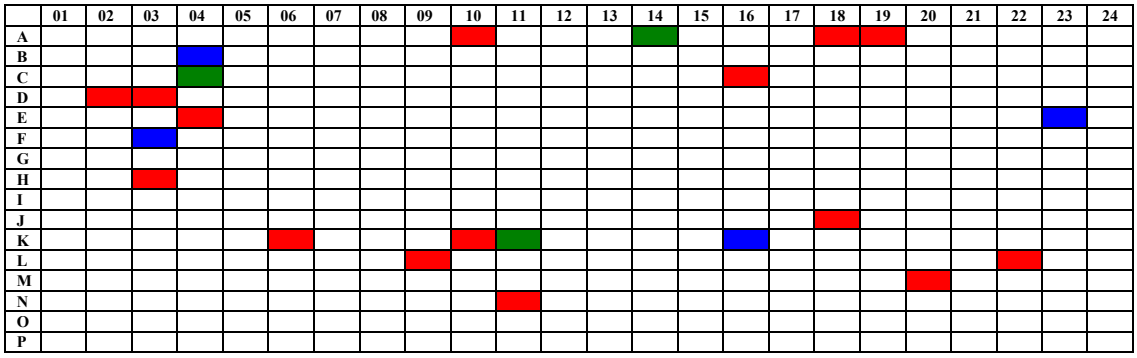

Figure 4.3 Results from the second three concentration dose-response screen

Compounds were dosed to cells using a three-fold dilution curve 20μM, 6μM, 2.2μM Compounds depicted in white predicted a double-digit micromolar IC50 value. Compounds that predicted an IC50 in HL60 cells greater than HL60/DOX are depicted in blue, compounds that predicted an IC50 in HL60/DOX cells greater than HL60 depicted in green, and compounds that predicted an IC50 equally potent in both cell lines are depicted in red.

Compound	IC_{50} in HL60	IC_{50} in HL60/DOX
1F03	11.2 ± 8	2.78 ± 2
1B04	3.90 ± 1	1.79 ± 0.2
1K16	2.11 ± 0.2	1.19 ± 0.5
1E23	11.3 ± 2	2.04 ± 0.5
1C04	N/A	4.21 ± 1
1K11	1.10 ± 0.03	12.2 ± 9
1A14	N/A	5.84 ± 0.3
1K10	1.78 ± 0.4	2.05 ± 0.2
1M20	1.77 ± 1	1.76 ± 0.6

Figure 4.4 Selected approximate IC_{50} values from a three dose response curve

Compounds were evaluated in a cell viability assay at 20, 6.66 and 2.22μM concentrations in HL60 and HL60/DOX cells. The IC_{50} (μM) was determined from the fit of a dose-response curve to the four-parameter dose-response equation (Eq. 2.1). Values

are an average of two independent experiments. Compounds 1C04 and 1A14 were too potent in HL60 cells to obtain accurate IC_{50} values.

4.2.3 Third screen - full dose response screening

The 22 compounds selected from the second screen were evaluated at 6 concentrations to estimate their IC_{50} values. Compounds exhibited low micromolar or high nanomolar IC_{50} values (Figure 4.5). Compounds 1E04 and 1L09 were too potent to reveal a dose response curve to fit to equation 2.1. Further testing is needed to produce accurate IC_{50} values of these compounds. Interestingly, compound 1D02 that exhibited potency in initial and secondary screening was inactive when screened for the full dose response. The inactivity could be due to compound degradation in the stock solution of DMSO. Without the initial structure of 1D02, it would be difficult to confirm any possible degradation products. With exception to 1E04, 1L09, and 1D02, all 19 compounds produced IC_{50} values within the range of detection by the cell viability assay. The compounds of most interest were those that proved to be at least two times more potent in HL60/DOX than in HL60: 1F03, 1H03, 1B04, 1L09, 1A10, 1J18, 1A19, 1M20, 1L22, and 1E23. The structures of these 22 compounds will be obtained from our collaborator to analyze structure activity relationships and to possibly identify a novel scaffold for chemotherapeutic drugs.

Compound	**IC_{50} in HL60**	**IC_{50} in HL60/DOX**	**$\frac{\text{HL60}}{\text{(HL60/DOX)}}$**

1D03	0.0264 ± 0.0003	0.0274 ± 0.002	1.0
1K10	2.44 ± 0.3	2.73 ± 0.2	0.9
1A18	0.814 ± 0.1	1.02 ± 0.2	0.8
1J18	0.719 ± 0.3	0.343 ± 0.2	2.1
1C04	0.118 ± 0.01	2.34 ± 0.1	0.1
1K06	0.0276 ± 0.003	0.0432 ± 0.01	0.6
1K11	0.730	2.75	0.3
1A14	0.223 ± 0.06	6.09 ± 3	0.04
1C16	0.418 ± 0.03	0.623 ± 0.1	0.7
1F03	8.12	2.96	2.7
1H03	0.654 ± 0.4	0.202 ± 0.1	3.2
1B04	5.15 ± 1	1.51 ± 0.1	3.4
1A10	0.661 ± 0.3	0.194 ± 0.1	3.4
1N11	0.823 ± 0.09	0.552 ± 0.1	1.5
1K16	2.05 ± 0.7	1.12 ± 0.1	1.8
1A19	1.96 ± 0.1	0.465 ± 0.1	4.2
1M20	2.38 ± 0.2	1.07 ± 0.2	2.2
1L22	0.728 ± 0.2	0.255 ± 0.1	2.9
1E23	10.5	2.28	4.6

Figure 4.5 In vitro IC_{50} values (µM)

Cell viability was measured using a three-fold dilution curve using 6 concentrations starting at 20µM, 6.66µM, or 2.22µM based on results obtained from the second screen. Each experiment was performed twice by independent individuals, except for compounds 1F03, 1K11, and 1E23 due to limited compound supply. Values are an average of the two experiments and are in µM concentrations. Technical triplicates were performed within each experiment. HL60/(HL60/DOX) is the ratio between the respective IC_{50} values.

4.3 Conclusion

Several compounds were discovered from the three cell viability screens. The 21 compounds discovered exhibited low to submicromolar IC_{50} values in both HL60 and HL60/DOX cell lines. Of the 21 compounds five compounds decreased cell viability in HL60 cells greater than HL60/DOX cells, ten compounds decreased cell viability in

HL60/DOX cells greater than HL60 cells, and six were equipotent in both cell lines. The structures of these compounds need to be obtained from our collaborator. Structures will be explored for novel scaffolds and possible modifications to increase potency. Lead compounds will be validated in authenticated HL60/DOX cells and screened in other drug resistant cancer cell lines.

4.4 Materials and methods

Compounds were obtained in a 384 well format from the lab of Dr. Rohan Davis at Griffith University. All commercial reagents and anhydrous solvents were purchased from vendors and were used without further purification or distillation unless otherwise stated.

4.4.1 Cell cultures

HL60 was purchased from ATCC. HL60/DOX was developed from HL60 upon exposure to doxorubicin. Cell lines were grown in RPMI 1640 media (ATCC) supplemented with 10% FBS and incubated at 37 °C under 5% CO_2 in air.

4.4.2 Cell viability measurement

Cytotoxicity was assessed by way of the CellTiter-Blue cell viability assay kit (Promega, Madison, WI) (see Section 2.4.6).[26] Similarly data were plotted and fit (Equation 2.1) to obtain the IC_{50} of each inhibitor.

References

1. Perez-Tomas, R., Multidrug resistance: Retrospect and prospects in anti-cancer drug treatment. *Current Medicinal Chemistry* **2006,** *13* (16), 1859-1876.

2. Gottesman, M. M., Mechanisms of cancer drug resistance. *Annual Review of Medicine* **2002,** *53*, 615-627.

3. Holohan, C.; Van Schaeybroeck, S.; Longley, D. B.; Johnston, P. G., Cancer drug resistance: an evolving paradigm. *Nature Reviews Cancer* **2013,** *13* (10), 714-726.

4. Stewart, T. A.; Yapa, K. T. D. S.; Monteith, G. R., Altered calcium signaling in cancer cells. *Biochimica et Biophysica Acta (BBA) - Biomembranes* (0); Orrenius, S.; Zhivotovsky, B.; Nicotera, P., Regulation of cell death: The calcium-apoptosis link. *Nature Reviews Molecular Cell Biology* **2003,** *4* (7), 552-565.

5. Arbabian, A.; Brouland, J.-P.; Gelebart, P.; Kovacs, T.; Bobe, R.; Enouf, J.; Papp, B., Endoplasmic reticulum calcium pumps and cancer. *Biofactors* **2011,** *37* (3), 139-149.

6. Wootton, L. L.; Michelangeli, F., The effects of the phenylalanine 256 to valine mutation on the sensitivity of sarcoplasmic/endoplasmic reticulum Ca2+ ATPase (SERCA) Ca2+ pump isoforms 1, 2, and 3 to thapsigargin and other inhibitors. *Journal of Biological Chemistry* **2006,** *281* (11), 6970-6976.

7. Mekahli, D.; Bultynck, G.; Parys, J. B.; De Smedt, H.; Missiaen, L., Endoplasmic-Reticulum Calcium Depletion and Disease. *Cold Spring Harbor Perspectives in Biology* **2011,** *3* (6).

8. Bergner, A.; Huber, R. M., Regulation of the Endoplasmic Reticulum Ca2+-Store in Cancer. *Anti-Cancer Agents in Medicinal Chemistry* **2008,** *8* (7), 705-709.

9. Joseph, S. K.; Hajnoczky, G., IP3 receptors in cell survival and apoptosis: Ca2+ release and beyond. *Apoptosis* **2007,** *12* (5), 951-968.

10. Janssen, K.; Horn, S.; Niemann, M. T.; Daniel, P. T.; Schulze-Osthoff, K.; Fischer, U., Inhibition of the ER Ca2+ pump forces multidrug-resistant cells deficient in Bak and Bax into necrosis. *Journal of Cell Science* **2009,** *122* (24), 4481-4491.

11. Hu, Q. L.; Chang, J. L.; Tao, L. T.; Yan, G. L.; Xie, M. C.; Wang, Z., Endoplasmic reticulum mediated necrosis-like apoptosis of Hela cells induced by Ca2+ oscillation. *Journal of Biochemistry and Molecular Biology* **2005,** *38* (6), 709-716.

12. Kitsis, R. N.; Molkentin, J. D., Apoptotic cell death "Nixed" by an ER-mitochondrial necrotic pathway. *Proceedings of the National Academy of Sciences of the United States of America* **2010,** *107* (20), 9031-9032.

13. Hoyer-Hansen, M.; Jaattela, M., Connecting endoplasmic reticulum stress to autophagy by unfolded protein response and calcium. *Cell Death and Differentiation* **2007,** *14* (9), 1576-1582.

14. Hoyer-Hansen, M.; Bastholm, L.; Szyniarowski, P.; Campanella, M.; Szabadkai, G.; Farkas, T.; Bianchi, K.; Fehrenbacher, N.; Elling, F.; Rizzuto, R.; Mathiasen, I. S.; Jaattela, M., Control of macroautophagy by calcium, calmodulin-dependent kinase kinase-beta, and Bcl-2. *Molecular Cell* **2007,** *25* (2), 193-205.

15. Nakagawa, T.; Zhu, H.; Morishima, N.; Li, E.; Xu, J.; Yankner, B. A.; Yuan, J. Y., Caspase-12 mediates endoplasmic-reticulum-specific apoptosis and cytotoxicity by amyloid-beta. *Nature* **2000,** *403* (6765), 98-103.

16. Gou, W.-F.; Niu, Z.-F.; Zhao, S.; Takano, Y.; Zheng, H.-C., Aberrant SERCA3 expression during the colorectal adenoma-adenocarcinoma sequence. *Oncology Reports* **2014,** *31* (1), 232-240.

17. Wang, M.; Kaufman, R. J., The impact of the endoplasmic reticulum protein-folding environment on cancer development. *Nature Reviews Cancer* **2014,** *14* (9), 581-597.

18. Schonthal, A. H., Endoplasmic reticulum stress and autophagy as targets for cancer therapy. *Cancer Letters* **2009,** *275* (2), 163-169.

19. Michelangeli, F.; East, J. M., A diversity of SERCA Ca2+ pump inhibitors. *Biochemical Society Transactions* **2011,** *39*, 789-797.

20. Inesi, G.; Sagara, Y., SPECIFIC INHIBITORS OF INTRACELLULAR CA2+ TRANSPORT ATPASES. *Journal of Membrane Biology* **1994,** *141* (1), 1-6.

21. Anand, P.; Kunnumakkara, A. B.; Newman, R. A.; Aggarwal, B. B., Bioavailability of curcumin: Problems and promises. *Molecular Pharmaceutics* **2007,** *4* (6), 807-818.

22. Fan, L.; Li, A.; Li, W.; Cai, P.; Yang, B.; Zhang, M.; Gu, Y.; Shu, Y.; Sun, Y.; Shen, Y.; Wu, X.; Hu, G.; Wu, X.; Xu, Q., Novel role of Sarco/endoplasmic reticulum calcium ATPase 2 in development of colorectal cancer and its regulation by F36, a curcumin analog. *Biomedicine & Pharmacotherapy* **2014,** *68* (8), 1141-1148.

23. Wong, V. K. W.; Li, T.; Law, B. Y. K.; Ma, E. D. L.; Yip, N. C.; Michelangeli, F.; Law, C. K. M.; Zhang, M. M.; Lam, K. Y. C.; Chan, P. L.; Liu, L., Saikosaponin-d, a novel SERCA inhibitor, induces autophagic cell death in apoptosis-defective cells. *Cell Death & Disease* **2013,** *4*.

24. Li, W.; Ouyang, Z.; Zhang, Q.; Wang, L.; Shen, Y.; Wu, X.; Gu, Y.; Shu, Y.; Yu, B.; Sun, Y.; Xu, Q., SBF-1 exerts strong anticervical cancer effect through inducing endoplasmic reticulum stress-associated cell death via targeting sarco/endoplasmic reticulum Ca2+-ATPase 2. *Cell Death Dis* **2014,** *5*, e1581.

25. Hermanson, D.; Addo, S. N.; Bajer, A. A.; Marchant, J. S.; Das, S. G. K.; Srinivasan, B.; Al-Mousa, F.; Michelangeli, F.; Thomas, D. D.; LeBien, T. W.; Xing, C., Dual Mechanisms of sHA 14-1 in Inducing Cell Death through Endoplasmic Reticulum and Mitochondria. *Molecular Pharmacology* **2009,** *76* (3), 667-678.

26. Das, S. G.; Doshi, J. M.; Tian, D.; Addo, S. N.; Srinivasan, B.; Hermanson, D. L.; Xing, C., Structure-Activity Relationship and Molecular Mechanisms of Ethyl 2-Amino-4-(2-ethoxy-2-oxoethyl)-6-phenyl-4H-chromene-3-carboxylate (sHA 14-1) and Its Analogues. *Journal of Medicinal Chemistry* **2009,** *52* (19), 5937-5949.

27. Das, S. G.; Srinivasan, B.; Hermanson, D. L.; Bleeker, N. P.; Doshi, J. M.; Tang, R.; Beck, W. T.; Xing, C., Structure-Activity Relationship and Molecular Mechanisms of Ethyl 2-Amino-6-(3,5-dimethoxyphenyl)-4-(2-ethoxy-2-oxoethyl)-4H-chromene-3-ca rboxylate (CXL017) and Its Analogues. *Journal of Medicinal Chemistry* **2011,** *54* (16), 5937-5948.

28. Bleeker, N. P.; Cornea, R. L.; Thomas, D. D.; Xing, C., A Novel SERCA Inhibitor Demonstrates Synergy with Classic SERCA Inhibitors and Targets Multidrug-Resistant AML. *Molecular Pharmaceutics* **2013,** *10* (11), 4358-4366.

29. Aridoss, G.; Zhou, B.; Hermanson, D. L.; Bleeker, N. P.; Xing, C., Structure-Activity Relationship (SAR) Study of Ethyl 2-Amino-6-(3,5-dimethoxyphenyl)-4-(2-ethoxy-2-oxoethyl)-4H-chromene-3-ca rboxylate (CXL017) and the Potential of the Lead

against Multidrug Resistance in Cancer Treatment. *Journal of Medicinal Chemistry* **2012,** *55* (11), 5566-5581.

30. Papp, B.; Brouland, J.-P.; Arbabian, A.; Gelebart, P.; Kovacs, T.; Bobe, R.; Enouf, J.; Varin-Blank, N.; Apati, A., Endoplasmic reticulum calcium pumps and cancer cell differentiation. *Biomolecules* **2012,** *2* (1), 165-86.

31. Monteith, G. R.; McAndrew, D.; Faddy, H. M.; Roberts-Thomson, S. J., Calcium and cancer: targeting Ca2+ transport. *Nature Reviews Cancer* **2007,** *7* (7), 519-530.

32. Parkash, J.; Asotra, K., Calcium wave signaling in cancer cells. *Life Sciences* **2010,** *87* (19-22), 587-595.

33. Xu, X.-y.; Gou, W.-f.; Yang, X.; Wang, G.-l.; Takahashi, H.; Yu, M.; Mao, X.-y.; Takano, Y.; Zheng, H.-c., Aberrant SERCA3 expression is closely linked to pathogenesis, invasion, metastasis, and prognosis of gastric carcinomas. *Tumor Biology* **2012,** *33* (6), 1845-1854.

34. Monteith, G. R.; Davis, F. M.; Roberts-Thomson, S. J., Calcium Channels and Pumps in Cancer: Changes and Consequences. *Journal of Biological Chemistry* **2012,** *287* (38), 31666-31673.

35. Prasad, V.; Boivin, G. P.; Miller, M. L.; Liu, L. H.; Erwin, C. R.; Warner, B. W.; Shull, G. E., Haploinsufficiency of Atp2a2, encoding the sarco(endo)plasmic reticulum Ca2+-ATPase isoform 2 Ca-2 pump, predisposes mice to squamous cell tumors via a novel mode of cancer susceptibility. *Cancer Research* **2005,** *65* (19), 8655-8661.

36. Akl, H.; Vervloessem, T.; Kiviluoto, S.; Bittremieux, M.; Parys, J. B.; De Smedt, H.; Bultynck, G., A dual role for the anti-apoptotic Bcl-2 protein in cancer: Mitochondria

versus endoplasmic reticulum. *Biochimica Et Biophysica Acta-Molecular Cell Research* **2014,** *1843* (10), 2240-2252.

37. Yano, M.; Ikeda, Y.; Matsuzaki, M. U., Altered intracellular Ca2+ handling in heart failure. *Journal of Clinical Investigation* **2005,** *115* (3), 556-564.

38. Dubois, C.; Vanden Abeele, F.; Sehgal, P.; Olesen, C.; Junker, S.; Christensen, S. B.; Prevarskaya, N.; Moller, J. V., Differential effects of thapsigargin analogues on apoptosis of prostate cancer cells Complex regulation by intracellular calcium. *Febs Journal* **2013,** *280* (21), 5430-5449.

39. Denmeade, S. R.; Isaacs, J. T., The SERCA pump as a therapeutic target - Making a "smart bomb" for prostate cancer. *Cancer Biology & Therapy* **2005,** *4* (1), 14-22.

40. Das, S. G.; Hermanson, D. L.; Bleeker, N.; Lowman, X.; Li, Y.; Kelekar, A.; Xing, C., Ethyl 2-Amino-6-(3,5-dimethoxyphenyl)-4-(2-ethoxy-2-oxoethyl)-4H-chromene-3-ca rboxylate (CXL017): A Novel Scaffold That Resensitizes Multidrug Resistant Leukemia Cells to Chemotherapy. *Acs Chemical Biology* **2013,** *8* (2), 327-335.

41. Martin, R.; Buchwald, S. L., Palladium-Catalyzed Suzuki-Miyaura Cross-Coupling Reactions Employing Dialkylbiaryl Phosphine Ligands. *Accounts of Chemical Research* **2008,** *41* (11), 1461-1473.

42. Hu, D.-F.; Weng, C.-M.; Hong, F.-E., Preparation of New Buchwald-Type Secondary Phosphine Oxide Ligands and Applications in Suzuki-Miyaura Reactions. *Organometallics* **2011,** *30* (5), 1139-1147.

43. Ishiyama, T.; Itoh, Y.; Kitano, T.; Miyaura, N., Synthesis of arylboronates via the palladium(O)-catalyzed cross-coupling reaction of tetra(alkoxo)diborons with aryl triflates. *Tetrahedron Letters* **1997,** *38* (19), 3447-3450.

44. Molander, G. A.; Trice, S. L. J.; Kennedy, S. M., Scope of the Two-Step, One-Pot Palladium-Catalyzed Borylation/Suzuki Cross-Coupling Reaction Utilizing Bis-Boronic Acid. *Journal of Organic Chemistry* **2012,** *77* (19), 8678-8688.

45. Giroux, A.; Han, Y. X.; Prasit, P., One pot biaryl synthesis via in situ boronate formation. *Tetrahedron Letters* **1997,** *38* (22), 3841-3844.

46. Ishiyama, T.; Murata, M.; Miyaura, N., PALLADIUM(O)-CATALYZED CROSS-COUPLING REACTION OF ALKOXYDIBORON WITH HALOARENES - A DIRECT PROCEDURE FOR ARYLBORONIC ESTERS. *Journal of Organic Chemistry* **1995,** *60* (23), 7508-7510.

47. MorenoManas, M.; Perez, M.; Pleixats, R., Palladium-catalyzed Suzuki-type self-coupling of arylboronic acids. A mechanistic study. *Journal of Organic Chemistry* **1996,** *61* (7), 2346-2351.

48. Miyaura, N.; Suzuki, A., PALLADIUM-CATALYZED CROSS-COUPLING REACTIONS OF ORGANOBORON COMPOUNDS. *Chemical Reviews* **1995,** *95* (7), 2457-2483.

49. Geurink, P. P.; Prely, L. M.; van der Marel, G. A.; Bischoff, R.; Overkleeft, H. S., Photoaffinity Labeling in Activity-Based Protein Profiling. *Activity-Based Protein Profiling* **2012,** *324*, 85-113.

50. Chen, I.; Ting, A. Y., Site-specific labeling of proteins with small molecules in live cells. *Current Opinion in Biotechnology* **2005,** *16* (1), 35-40.

51. Dorman, G.; Prestwich, G. D., Using photolabile ligands in drug discovery and development. *Trends in Biotechnology* **2000,** *18* (2), 64-77.

52. Sakurai, K.; Ozawa, S.; Yamada, R.; Yasui, T.; Mizuno, S., Comparison of the Reactivity of Carbohydrate Photoaffinity Probes with Different Photoreactive Groups. *Chembiochem* **2014,** *15* (10), 1399-1403.

53. Rizk, M. S.; Shi, X. F.; Platz, M. S., Lifetimes and reactivities of some 1,2-didehydroazepines commonly used in photoaffinity labeling experiments in aqueous solutions. *Biochemistry* **2006,** *45* (2), 543-551.

54. Smith, E.; Collins, I., Photoaffinity labeling in target- and binding-site identification. *Future Medicinal Chemistry* **2015,** *7* (2), 159-183.

55. Best, M. D., Click Chemistry and Bioorthogonal Reactions: Unprecedented Selectivity in the Labeling of Biological Molecules. *Biochemistry* **2009,** *48* (28), 6571-6584.

56. Stokes, D. L.; Green, N. M., 3-DIMENSIONAL CRYSTALS OF CAATPASE FROM SARCOPLASMIC-RETICULUM - SYMMETRY AND MOLECULAR PACKING. *Biophysical Journal* **1990,** *57* (1), 1-14.

57. Sumranjit, J.; Chung, S. J., Recent Advances in Target Characterization and Identification by Photoaffinity Probes. *Molecules* **2013,** *18* (9), 10425-10451.

58. Voskresenska, V.; Wilson, R. M.; Panov, M.; Tarnovsky, A. N.; Krause, J. A.; Vyas, S.; Winter, A. H.; Hadad, C. M., Photoaffinity Labeling via Nitrenium Ion Chemistry: Protonation of the Nitrene Derived from 4-Amino-3-nitrophenyl Azide to Afford Reactive Nitrenium Ion Pairs. *Journal of the American Chemical Society* **2009,** *131* (32), 11535-11547.

59. Barral, K.; Moorhouse, A. D.; Moses, J. E., Efficient conversion of aromatic amines into azides: A one-pot synthesis of triazole linkages. *Organic Letters* **2007,** *9* (9), 1809-1811.

60. Mueller, B.; Zhao, M.; Negrashov, I. V.; Bennett, R.; Thomas, D. D., SERCA structural dynamics induced by ATP and calcium. *Biochemistry* **2004,** *43* (40), 12846-12854.

61. Macarron, R.; Banks, M. N.; Bojanic, D.; Burns, D. J.; Cirovic, D. A.; Garyantes, T.; Green, D. V. S.; Hertzberg, R. P.; Janzen, W. P.; Paslay, J. W.; Schopfer, U.; Sittampalam, G. S., Impact of high-throughput screening in biomedical research. *Nature Reviews Drug Discovery* **2011,** *10* (3), 188-195.

62. Vassilev, L. T.; Kazmer, S.; Marks, I. M.; Pezzoni, G.; Sala, F.; Mischke, S. G.; Foley, L.; Berthel, S. J., Cell-based screening approach for antitumor drug leads which exploits sensitivity differences between normal and cancer cells: identification of two novel cell-cycle inhibitors. *Anti-Cancer Drug Design* **2001,** *16* (1), 7-17.

63. Balis, F. M., Evolution of anticancer drug discovery and the role of cell-based screening. *Journal of the National Cancer Institute* **2002,** *94* (2), 78-79.

64. Butcher, E. C., Can cell systems biology rescue drug discovery? *Systems Biology: Applications and Perspectives* **2007,** *61*, 153-172.

65. Kemnitzer, W.; Drewe, J.; Jiang, S. C.; Zhang, H.; Wang, Y.; Zhao, J. H.; Jia, S. J.; Herich, J.; Labreque, D.; Storer, R.; Meerovitch, K.; Bouffard, D.; Rej, R.; Denis, R.; Blais, C.; Lamothe, S.; Attardo, G.; Gourdeau, H.; Tseng, B.; Kasibhatla, S.; Cai, S. X., Discovery of 4-aryl-4H-chromenes as a new series of apoptosis inducers using a cell- and

caspase-based high-throughput screening assay. 1. Structure-activity relationships of the 4-aryl group. *Journal of Medicinal Chemistry* **2004,** *47* (25), 6299-6310.

66. Mann, J., Natural products in cancer chemotherapy: past, present and future. *Nature Reviews Cancer* **2002,** *2* (2), 143-148.

67. Harvey, A. L.; Edrada-Ebel, R.; Quinn, R. J., The re-emergence of natural products for drug discovery in the genomics era. *Nature Reviews Drug Discovery* **2015,** *14* (2), 111-129.

68. Cragg, G. M.; Newman, D. J., Plants as a source of anti-cancer agents. *Journal of Ethnopharmacology* **2005,** *100* (1-2), 72-79.

69. Lipinski, C. A.; Lombardo, F.; Dominy, B. W.; Feeney, P. J., Experimental and computational approaches to estimate solubility and permeability in drug discovery and development settings. *Advanced Drug Delivery Reviews* **2012,** *64*, 4-17.